universität wien

DIPLOMARBEIT

Titel der Diplomarbeit

Fluorescent virus-like particles as novel platform to identify immune-receptor/ligand interactions on leukocyte subsets

angestrebter akademischer Grad

Magister der Naturwissenschaften (Mag. rer.nat.)

Verfasser:	MANTA, Calin-Petru
Matrikel-Nummer:	0506536
Studienzweig (lt. Studienblatt):	(A441) Mikrobiologie/Genetik
Betreuer:	Ao.Univ. Prof. Dr. Winfried F. Pickl
Wien, im Mai 2009	Institut für Immunologie, Zentrum für Physiologie, Pathophysiologie und Immunologie, Medizinische Universität Wien

Zusammenfassung

In der vorliegenden Arbeit haben wir uns die Frage gestellt, ob selektive virusähnliche Partikel (VLP) mit einem fluoreszierenden Protein ausgestattet werden können, um damit entsprechende Zielzellen identifizieren zu können. Unsere Arbeitsgruppe hat in der Vergangenheit gezeigt, dass VLP, welche vom Moloney Mäuse Leukämie Viruses (MoMLV) abstammen, mit Immunmodulatoren oder Zytokinen der Wahl ausgestattet werden können. Derartige VLP können polyklonale oder aber auch eine immunspezifische T-Zell Antwort induzieren. Partikel, die zusätzlich mit fluoreszierenden Proteinen ausgestattet werden und die einen Liganden für einen entsprechenden Oberflächen-Rezeptor exprimieren, können dazu verwendet werden, um entsprechende Zielzellen zu detektieren. In der vorliegenden Arbeit wurde das grünfluoreszierende Protein (GFP) mit dem Matrix Protein (MA) des MoMLV genetisch verknüpft. MA::GFP wird in transfizierten Zellen in den sogenannten “lipid rafts“ angereichert. Als Produzentenzelllinie wurden die mit dem MA::GFP stabil transfizierten HEK-293 Zellen etabliert. Die transiente Transfektion der HEK-293 MA::GFP Zellen mit Kapsidproteinen führte zur Sekretion von fluoreszierenden Partikeln, welche wir als Fluorosomen (FS) bezeichnen. FS wurden aus den Überständen der HEK-293 MA::GFP Zellen mittels Ultrazentrifugation angereichert und mit entsprechenden Zielzellen inkubiert. Die derartig behandelten Zellen wurden anschließend mittels Durchflusszytometrie analysiert. Die FS wurden mit GPI-verankerten Liganden dekoriert was in transient transfizierten HEK-293 Zellen erreicht wurde. FS die mit IL-2::GPI ausgestattet wurden, konnten erfolgreich zum Nachweis von HT-2 Zellen verwendet werden, die den Maus IL-2 Rezeptor konstitutiv auf ihrer Zelloberfläche exprimieren. Des Weitern konnte gezeigt werden, dass FS auch für den Nachweis von IL-2 Rezeptorkomponenten, exprimiert auf HEK-293 Zellen, geeignet sind. Es konnte auch gezeigt werden, dass auf FS auch komplexe Strukturen verankert werden können, indem wir einen kompletten IL-2 Rezeptor transient transfiziert haben um membranständiges IL-2::GPI nachweisen zu können. Des Weitern konnte gezeigt werden, dass IL-2::GPI FS und IL-7::GPI FS, aktivierte humane T-Lymphozyten des peripheren Blutes identifizieren können. Schlussendlich wurde auch der Nachweis erbracht, dass maligne Zellen von Patienten mit chronischer lymphatischer Leukämie mit IL-2::GPI FS identifiziert werden können. Die Schlussfolgerung dieser Arbeit ist, dass FS nützliche Hilfsmittel darstellen, die zum

Nachweis von mono- oder polyvalenten immunologischen Rezeptor/Ligand Interaktion genutzt werden können.

Abstract

Moloney murine leukemia virus (MoMLV) derived particles decorated with immunomodulators and cytokines can be used to influence polyclonal and antigen-specific T cell responses. By targeting fluorescent dyes to these particles, the interaction between the particle-borne ligands and their respective receptors on the cell surface of target cells can be visualized. For that purpose, the green fluorescent protein (GFP) was fused to the matrix protein (MA) of MoMLV, which leads to lipid raft targeting and in consequence to the incorporation into virus-like particles (VLP). In a first step, HEK-293 cells stably transfected with MA::GFP were established as VLP producer cells. Upon transfection with MoMLV core proteins the production of fluorescent VLP- designated as fluorosome (FS) - was induced. FS were purified from the supernatant of producer cells by ultracentrifugation and used for staining of various target cells in a similar way as antibodies in flow cytometric analyses. Decoration with specific ligands was achieved by co-transfection of GPI-anchored molecules into the producer cell. In proof of principle experiments, FS decorated with IL-2::GPI were used to stain murine HT-2 cells, which constitutively express the murine IL-2 receptor. In these experiments the staining capacity of FS was evaluated. Furthermore IL-2::GPI FS were used to stain HEK-293 cells transfected with IL-2 receptor components and *vice versa*. It was also shown that FS decorated with IL-2::GPI or IL-7::GPI can stain human peripheral blood mononuclear cells (PBMC) from healthy individuals and chronic lymphatic leukemia (CLL) patients. In conclusion FS with membrane-targeted fluorescent proteins are useful tools for assessing mono- and multi-subunit immune-receptor/ligand interactions.

Danksagung

Ich möchte meinen Eltern, Cristina und Claudiu Manta danken, die mich immer unterstützt haben, an mich geglaubt haben und immer hinter mir standen.

Ich möchte mich bei meinem offiziellen Betreuer ao. Univ. Prof. Dr. Winfried Pickl bedanken, der mir die Diplomarbeit ermöglicht hat, mich hervorragend bereute und mich für die medizinische Wissenschaft begeistern konnte.

Ich möchte mich bei meinem inoffiziellen Betreuer und Kollegen Hans Küng bedanken, der mir das praktische Arbeiten und auch alle "Tricks und Kniffe" im Labor beigebracht hat und mit dem ich nicht nur hervorragend und gern zusammen gearbeitet habe sonder mit dem ich auch sonst viel "Spaß" hatte.

Des Weitern möchte ich mich bei Klaus Schmetterer - "der Kaiser" - bedanken, der nicht nur ein hervorragender Wissenschaftler ist, sonder auch bald Arzt sein wird, und der mir beim korrigieren der Arbeit geholfen hat.

Auch bei Daniela Haiderer möchte ich mich bedanken, die immer ein offenes Ohr hatte sowohl in wissenschaftlichen als auch in menschlichen Belangen und mir sehr beim verfassen der Arbeit geholfen hat.

Bei meiner Kollegin Alina Neunkirchner, die mich durch ihren Fleiß immer angespornt und durch ihr sonniges Gemüht aufgeheitert hat, möchte ich mich besonders bedanken.

Auch meiner Kollegin Victoria Leb gilt mein Dank, für ihre vielen guten und nützlichen Tipps, die in meine Arbeit eingeflossen sind.

„Last but not least" möchte ich mich bei Karina Schuch bedanken, die mir durch ihre Gewissenhaftigkeit und Lebensfreude stets ein Vorbild war - und ist.

Table of contents

1. Introduction

In the past it was shown that virus-like particles (VLP) can be used as innovative platform for the generation of immuno-stimulatory (immunosomes) and immuno-modulatory (anergosomes) particles. (1-3) Studies using immunosomes, demonstrated the stimulation of T cells with cell-free VLP expressing the primary signal in form of a surrogate TCR/CD3 ligand (OKT3scFv) and the costimulatory second signal CD80, which lead to polyclonal activation of T cells. (1) Further studies incorporated human interleukin-2 (hIL-2), hIL-4 or human granulocyte-macrophages colony-stimulating factor (hGM-CSF) but also murine IL-2 into VLP which lead to stimulation of T cells and monocytes. (2) The experiments in the past concentrated predominantly on immunoreceptor effects on cells of the immune system, which lead us to speculate if it would be possible to visualize these interactions. First we tested if it would be possible to target recombinant fluorescent proteins of Cnidarian origin corresponding to the green fluorescent protein (GFP) of *Aequorea victoria* or mcherry of *Discosoma sp*. (4-6) to the membrane of virus-like particles (VLP). Targeting of the fluorochromes was achieved by fusing them to the matrix protein (MA) of Moloney murine leukemia virus (MoMLV). (7, 8) The MA protein gets posttranslationally modified followed by targeting into the plasma membrane, with fused GFP or mcherry. This forms the basis for the production of our fluorescent VLP or “fluorosomes” (FS) based on MA::GFP (green) or MA::mCherry (red). (9, 10) Stably transfected human embryonic kidney (HEK)-293 cells expressing MA::GFP or MA::mCherry which is an immortalized cell type have been used as producer cell. The decoration of FS with molecules of choice can be achieved by fusion of the respective ectodomains with human Fc gamma receptor III (CD16b), which possesses a well-described glycosyl phosphatidyl inositol (GPI) anchor acceptor sequence. (2) The constructs used in this report are membrane bound human (h) interleukin (IL)-2::GPI, hIL-7::GPI and hIL-2 receptor–components. (2) Particle production was induced by co-expression of gag/pol (OGP) from MoMLV. (1) After purification, the FS can be used for staining of corresponding target cells.

1.1 Transport of membrane proteins

Protein translation and transport in the cell is segmented in two main pathways. The first pathway is the secretory pathway: Proteins are secreted to the endoplasmic reticulum (ER) already during translation. (11, 12) They pass the ER and the Golgi-network and some of them become post-translationally modified during this translocation. (11, 12) These modifications are for example glycosylation, acetylation, palmitoylation and myristoylation. (13, 14) After passing the Golgi-network members can either be secreted to the extracellular space to the lysosome or to the plasma-membrane. (11, 12) The second group of proteins is involved in cytosolic processes or organelle biogenesis. (11, 12) Proteins that are involved in organelle biogenesis lead to the formation and maturation of organelle components like membranes of the nucleus or the mitochondrion and cytosolic proteins are mainly involved in cellular enzymatic processes. (11, 12)

Generally, the first and most important step of protein targeting is the translation of the signal peptide. (11, 15) The coding mRNA contains on the 5`part a leader signal, which directs the protein in the cell. (11, 15) The leader peptide of transmembrane type I proteins is a highly hydrophobic sequence which is thus anchored into the ER membrane. (12, 15) The signal peptide is recognized by a protein complex that cuts this leader sequence and transports the translated protein into the lumen of the ER (Fig. 1). This complex is called the translocon. (15) The translocon consists of a signal recognition particle (SR) and a signal peptidase (SPC) that removes the leader sequence. (12, 15)

Due to the mechanism described above the translated protein is transported into the ER lumen. During this process the amino terminal part (N-terminus) is the first to be translocated into the ER lumen. (12, 15) These proteins (Fig.1) contain an approximately 22 amino acid (aa) long stop-transfer membrane anchor-sequence at the carboxy terminal part (C-terminus). (11) This is the signal that stops the transfer of the protein into the lumen of the ER. (11) Afterwards, the ribosome is disconnected from the translocon. (11) The fully translated protein is thereby anchored into the ER membrane. (11) Consequently, the C-terminus projects to the cytosol (outside of the ER lumen). (11, 12)

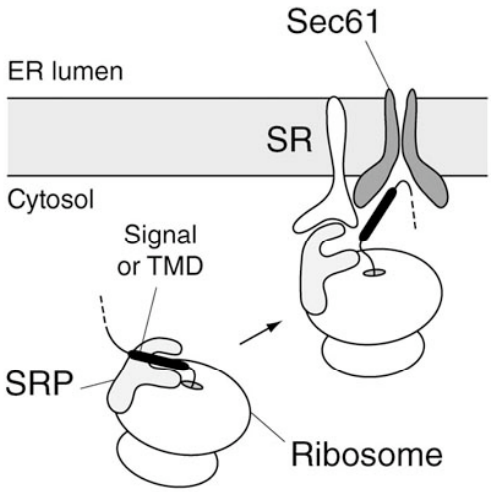

Figure 1. The transport of transmembrane proteins to the endoplasmic reticulum (ER). The translocon consists of Signal recognition particle (SRP), the SRP receptor (SR), Sec61 which form the tunnel, TRAM is required for some proteins and the signal peptidase (SPC). (15)
from: Ramanujan S. Hegde and Sang-Wook Kang; (2008) J Cell Biol. 182(2): 225–232

1.1.1 Post-translational modification

The ER and Golgi-network are responsible for post-translational modifications of proteins. (12) Post-translational modifications include generation of disulfide bonds, controlled folding of proteins with help of chaperons, attachment of carbohydrates, cleavage of pre-forms, connection to protein complexes and lipid modifications. (11, 15) The main part of the post-translational modifications occurs in the ER. (11) The environment in the ER facilitates the reduction of sulfide groups to their oxidized conformation, which leads to the generation of disulfide bonds. (11) Disulfide bonds are very important for protein stability and also for the formation of protein complexes. (11, 15) Furthermore, the ER contains numerous chaperons that are responsible for the formation of correct protein conformation. Some of these chaperons are for example the Protein Disulfide Isomerase (PDI), the heat shock protein 70 (Hsc70), Calnexin, Calreticulin and also the Peptidyl-Prolyl-Isomerase. (11, 15) The reassembling of protein complexes also takes place in the ER. (11, 12, 15) The next maturation step for a protein is the transport from the ER to the Golgi-network. Only appropriately folded proteins are able to leave the ER and enter into the Golgi-network for further modification. (11, 15, 16) Proteins with the wrong conformation form complexes with ER chaperons and are retained in the ER. (11, 13, 15, 16) These incorrectly folded proteins are

afterwards transported back from the ER into the cytosolic space and cleaved by the proteasome. (11, 13, 15, 16) Also incorrect translation processes lead to the formation of defective ribosomal products (DRiPs). (17) DRiPs of cytosolic proteins, are directly proteolysed by the proteasome. Secretory proteins, which are translated in the ER are transported back by the translocon into the cytosol followed by degradation in the proteasome. (17) The proteolysed peptides are transported into ER due to TAP and become then loaded onto MHC I. (17)
The inositol requiring enzyme 1 (IRE1) an ER-resident transmembrane protein is especially important. (11, 15, 16) This protein is responsible for the recognition of unfolded proteins. (11) IRE1 binds unfolded proteins and leads to splicing of the mRNA of the transcription factor HAC1. (11, 15, 16) HAC1 then enhances synthesis of chaperons for the refolding, when wrongly folded proteins accumulate. (11) If no proper folding can be achieved, proteins are ubiquitinylated, returned to the cytosol and cleaved by the proteasome. (11, 15, 16) Protein transport between the ER and cis-Golgi-network is mediated by so called shuttle vesicles. (11, 16) These shuttle vesicles contain the KDEL receptor. (11) All proteins containing a KDEL signal sequence are returned from cis- Golgi-network back to the ER. (11, 12, 15)

1.1.2 GPI-anchoring of type I membrane proteins

Transmembrane proteins are classified into two different groups dependent on their orientation and architecture in the plasma membrane (Fig.3). (18-20) In type I membrane proteins the N-terminus is localized extracellularly, while the C-terminus is in the cytosol. Type I membrane proteins typically have also a hydrophobic transmembrane domain. (19) Type II membrane proteins reveal the opposite orientation of C- and N-terminus relative to the plasma membrane compared to type I proteins. (15, 19) In general the orientation of the membrane proteins is achieved by the presence and localization of the protein leader signal sequence. (19)
As mentioned above, type I membrane proteins contain the leader signal sequence at the freshly synthesized N-terminus (Fig.2). (11, 15) The leader is recognized and removed by the SPC of the translocon. (15) The stop-transfer signal leads to ER transfer inhibition of the newly synthesized protein retaining it in the ER membrane. The translated type I membrane protein possesses a

characteristic C-terminal 21-26 amino acid (aa) length anchor consisting of a hydrophobic α-helix which anchors it to the ER membrane. (11, 15) The signal sequence of type II membrane proteins is not cleaved by SPC, instead it generates a loop relative to the tunnel proteins (Sec61) of the translocon which serves as anchor. (11, 15, 19) The consequence of this connection to the translocon is the opposite orientation of type II membrane proteins in respect to N- and C- terminus. (11, 15)

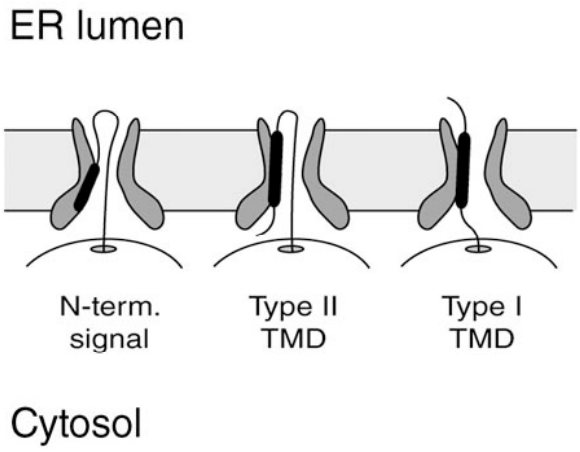

Figure 2. The localization of type I and type II proteins in the translocon.
adapted from: Ramanujan S. Hegde and Sang-Wook Kang; (2008) J Cell Biol. 182(2): 225–232

Further classifications include also type III and type IV transmembrane proteins. (19) The type III proteins (Fig.3) have a start-stop transfer sequence, the location of the proteins is dependent on the polarization of the α-helical domain that is anchored in the membrane. (19) Type III membrane proteins possess a non cleavable leader sequence like type I membrane proteins, but the electrical charge orientation is opposite to type II proteins. This orientation is reached through the polarized charges of the anchoring α-helix domain. (19) The α-helix of type II membrane proteins, is negatively charged relative to the N-terminus. (19) However, type III proteins, α-helical domain is positive in N-terminal direction. (19) The constitution of the membrane protein is affected through the charges within the α-helix. (19)

Type IV membrane proteins contain more than one α-helical domain (Fig.3), spanning the cell membrane. (19) These transmembrane proteins are

characterized by the numbers of the membrane spanning-domains. (15, 19) If the number of the spanning-domains is odd, the orientation of termini is opposite on the different sides related to the membrane (common type of structure 7-membrane passage), whereas to an even number the protein termini are arranged in the same direction (common type of structure 12-membrane passage). (15, 19)
GPI-anchored proteins belonging to type V membrane proteins are connected immediately after translation to a preformed GPI-anchor. The difference between α-helix anchored type I transmembrane proteins and GPI–anchored type V transmembrane proteins, except of their anchoring, is the signal during the translation that implicates the disconnection from the α-helix to the GPI-anchor. (11) The translated protein is associated with the ER membrane. (11) The N-terminus of the polypeptide is located in the ER lumen, the C-terminal α-helix is attached to the ER membrane and possesses the GPI-anchor attachment signal sequence which is required for the connection to the GPI-anchor. (11) An ER-endoprotease recognizes this sequence and couples it to a preformed GPI-anchor. (11) This ER endoprotease segregates by proteolysis the polypeptide from the hydrophobic membrane α-helix anchor and associates the free C-terminus of the protein with the free amino group of the GPI-anchor. (11, 21) This modification results in targeting of GPI-anchored membrane proteins into the lipid rafts.

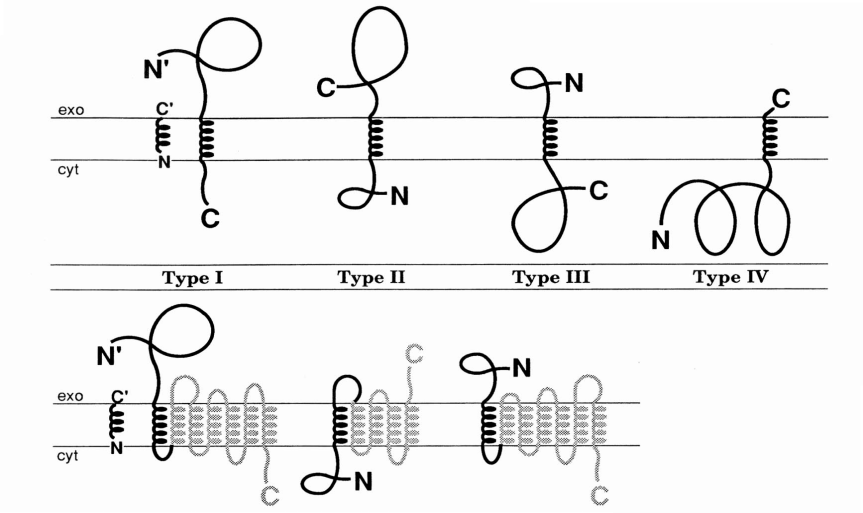

Figure 3. The order of transmembrane proteins.
from: Spiess M. (1995) FEBS Lett. 369:76

The GPI-anchor comprises a strictly conserved glycan core (mannose(α1-2) mannose(α1-6)mannose(α1-4)glucosamine(α1-6)myc-inositol). (22, 23) Moreover, numerous combinations of residues can be connected to the conserved glycan core molecule, which enhance the specificity of the anchoring, which is important for different receptors. (22, 24-26) The GPI-anchored protein is coupled through phosphoethanolamine to the C-termini of the GPI-anchor (Fig.4). (22, 24)

The connection of GPI-anchored proteins can be verified by incubation with phosphatidylinositol phospholipase C (PI-PLC) from *B. thuringiensis*. The consequence of the PI-PLC treatment is the release of GPI-anchored proteins. (11) The PI-PLC, that was purified from several bacteria (*Bacillus cereus, Staphylococcus aureus, Clostridium novyi* and also *Bacillus thuringiensis*), is able to cleave the bond between the glycerin and the inositol within the GPI-anchor (22, 27)

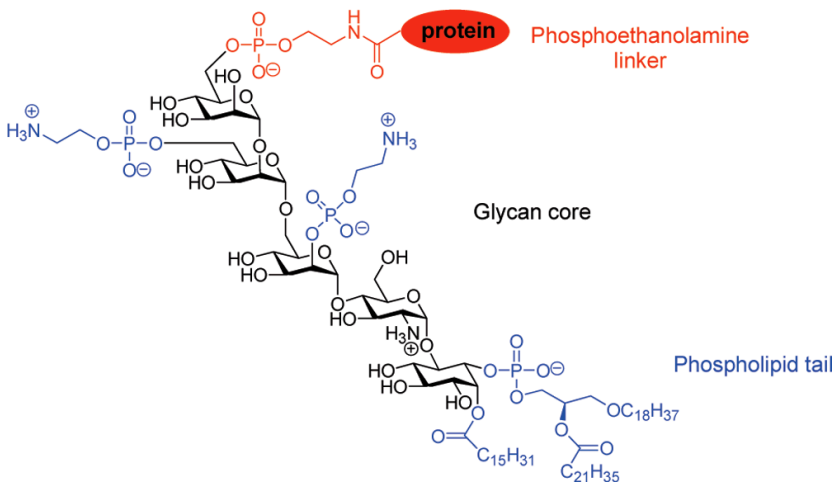

Figure 4. Typical structure of the GPI-anchor. The three domains of the GPI-anchor are: (I) (black) the glycan core backbone ; (II) (blue) phospholipid tail and (III) (red) phosphoethanolamine linker. The blue residues are variable.
from: Paulick MG, Bertozzi CR (2008) Biochemistry Review 47(27):6991-7000

1.1.3 Glycosylation in endoplasmic reticulum and Golgi-network

Glycosylation of proteins is happening in the Golgi-network and is also implemented in the ER. However, the first important glycosylation steps take already place in the ER. (11) During translation in the ER, proteins become N-

glycosylated. (11, 14) The glycosylation process is distinguished in N- or O-glycosylation. (11) During the O-glycosylation sugar residues are added consecutively to the protein and during the N-glycosylation process one oligosaccharide complex of different sugars is transferred to the receiver protein. (12, 14, 15) The sugar residues in the oligosaccharide complex are linked through N-glycosylic links. Some of the sugars are removed during the process of N-glycosylation, after the connection to the protein. (12, 14) The transfer of the oligosaccharide complex is dependent on the amino acid (aa) sequence of the protein (Asn-X-Ser or Asn-X-Thr, X is optional aa except of prolin). (11, 14, 28, 29) The oligosaccharide complex is connected to the asparagine of the protein. (11, 14) The oligosaccharide complex is composed of glucose $(Glc)_3$, mannose $(Man)_9$ and N-acetylglucosamine $(GlcNAc)_2$. (11, 14) The three glucose $(Glc)_3$ residues are removed during the transport process in the ER, so that only $(Man)_8$ $(GlcNAc)_2$ enter in the cis-Golgi-network. (11, 14) The oligosaccharide complex interacts with chaperons before entering into the Golgi-network, the right folding of the protein is controlled in this way. (11, 12, 14, 15)

The last post translational modifications of proteins happen in the Golgi-network. (12) The Golgi-network is segmented in three compartments, the cis, medial and trans-Golgi-network. (15) These compartments contain different specific enzymes that lead to addition or removal of monosaccharides. (11) The N-glycosylated protein ($(Man)_8$ $(GlcNAc)_2$) from the ER is transported into the cis-Golgi-network. (11) (14) The three mannose $(Man)_3$ residues are removed in the cis-Golgi-network, which leads to a new oligosaccharide structure $(Man)_5$ $(GlcNAc)_2$. (11, 14) Afterwards, the N-glycosylated protein is transported to the trans-Golgi-network, were several conversions of the connected sugar residues of the oligosaccharide complex take place. (11, 14) These conversions include the removal of $(Man)_2$ and the addition of three N-acetylglucosamine $(GlcNAc)_3$ residues and one fucose $(Fuc)_1$ molecule. (11, 12, 14) The new structure of the connected oligosaccharide complex is an assembly of $(GlcNAc)_3$ $(Man)_3$ $(GlcNAcGlc)_2$ $(Fuc)_1$. (11, 14) The enzymes in trans-Golgi-network perform two additional modifications in which three galactose $(Gal)_3$ and three N-acetylneuraminic acid $(NeuN5Ac)_3$ are connected with each of the three galactose $(Glc)_3$. (11, 12, 14)

GPI-anchored proteins are sorted, after all these maturation steps in the ER and the Golgi-network towards the plasma membrane. (11)

1.2 Lipid rafts - gateways for fluorosomes

The production of the fluorosomes (FS) and their decoration with GPI-anchored proteins is lipid raft dependent. Lipid rafts of the producer cells are meeting, anchoring, budding and secretion points for the decorated FS. (30)
The common definition for lipid rafts is that they are highly ordered cholesterol and sphingolipid enriched regions in the plasma membrane (14, 31, 32), organized and separated from the rest of the plasma membrane as microdomains. (33) The sphingolipids contain palmitol as main component, which is saturated. (21) The saturated hydrocarbons allow a very tightly packing of the self assembling lipid rafts in the bilayer. (22) The task of the cholesterol is to fill the empty space between the sphingolipids and this leads to a higher hydrophobicity and a high degree of order. (22, 31) The cholesterol is essential for the function and the formation of lipid rafts. Due, to this saturated components the lipid rafts are less fluid in comparison to the surrounding. (22, 31) Lipid rafts, are very important for cellular functions including trafficking of vesicles, signal transduction (22, 31, 32) and also as gateways for enveloped viruses. (1, 2) Further important characteristics of lipid rafts are their insolubility to detergents at 4°C. The condition for the detection of lipid raft targeted, GPI-anchored proteins is, the application of non-ionic detergent, for example Triton X-100 under strict low temperature (4°C) conditions. (22, 31, 32) Under this condition proteins associated with lipid rafts remain insoluble and can be isolated, by isopycnic sucrose gradient centrifugation. (22, 34)

1.3 Moloney murine leukemia virus as platform for fluorosomes

The ecotropic Moloney murine leukemia virus (MoMLV) is an enveloped retrovirus having two copies of viral RNA. (35-38) The advantages of MoMLV are, it´s easy handling, its tropism which makes it non-pathogenic for humans and the fact that it permits long-term transgenic expression in transduced cells. (35) The MoMLV genome contains three components, the core proteins (*gag*), the polymerase/ integrase (*pol*) and the envelope (*env*). (36, 37) The *env* encodes two polypeptides which are derived from a single precursor $gPr80^{env}$ which is proteolytically cleaved, into the 17-kDa transmembrane polypeptide (TM) and the 70-kDa surface glycoprotein protein (SU). (38-43) These two ENV proteins multimerize and build

up the spikes on the virus particle. (39-42) Palmitoylation is required for the targeting of the ENV proteins to the cell surface (38, 44-48) The SU proteins recognize respective receptor Ram-1 on the cell surface of the target cell (49, 50), the consequence is a conformational change in the spike, leading to membrane fusion and allowing virus-entry into the cell. (39, 51-53) MoMLV can be classified into five subgroups, depending of the SU protein. (39) MoMLV is a mouse and rat infectious virus that induces leukemia. (39, 54) Among others it was discovered that MoMLV has a leukemia inducing effect in p53 -/- mice, which developed tumors much faster as p53 +/- mice. (54).

The core proteins, also called "structural GAG" proteins have one common precursor the $p65^{gag}$. (55-59) The encoded structural proteins are the capsid protein (CA) p30, the nucleocapsid (NA) p10, the matrix protein (MA) p15 and p12. (55, 56, 60, 61)

The capsid proteins require myristylation at the N-terminal glycine, for targeting to the plasma membrane and for virus budding. (62-65) The pol genes encode the transcription components, the reverse transcriptase and the integrase of the virus. (60, 61)

In our experiments we used a vector system encoding only *gag* and *pol* (OGP) which upon transfection into the producer cell leads to the budding of non infectious virus-like particles (VLP). As a producer cell we used the human embryonic kidney cells, HEK-293, which is an embryonic kidney epithelial cell line transformed by sheared DNA of adenovirus type 5 (66) The transfection of HEK-293 cells with gag/pol OGP, leads to budding of the virus particles from the cell membrane. (1, 2, 35) The meeting point, but also the sites of budding for the MoMLV proteins are the lipid rafts of the plasma membrane. (1, 2, 35)

1.4 Interleukin-2 function

Interleukin-2 (IL-2) was initially discovered as a 15 kDa glycoprotein, in culture medium of lymphocytes that were stimulated with antigen or mitogen (67, 68) Because of it's T cell stimulating capacity it was named T cell growth factor (TCGF). The production of IL-2 requires an antigen presenting cell (APC) which activates T cell. APC takes up the pathogen, this leads to the presentation of the antigen on the MHC (in case of $CD4^+$ T cells on MHC II). (69, 70)

The APC migrates into the lymph node where it meets naive T cells and B cells. T cell and APC go through an initial recognition phase of the MHC and the peptide through the TCR (Signal 1). (69, 70) The recognition of the MHC and the peptide is the first step for the IL-2 activation. The second signal (Signal 2) is the T cell CD28 Receptor and the APC CD80 (B7.1) ligand that enhances and contributes to signal 1. (69, 70) Both signals are required for sustained IL-2 induction in T cells, which leads to activation and proliferation. (67)

The Lck kinase (Src family) which is coupled to the CD4 molecule (co-receptor) phosphorylates the immunoreceptor tyrosine-based activation motif (ITAM) domains of the CD3 and the ζ chains. (69, 70) ZAP 70 (Syk family) phosphorylates LAT adapter protein which is a signalling platform. (69, 70) Three main events, are activated from the phosphorylated LAT protein, the MAP kinase cascade, the opening of the Ca^{2+} channels and the recruitment of diacylglycerol (DAG). (69, 70) The mentioned events lead to the recruitment of transcription factors which initiate IL-2 transcription. (69, 70) The first pathway, the MAP kinase cascade involving the upstream factors Grb2 and Sos (heterodimer), leads to phosphorylation of monomeric Ras protein. (69, 70) Ras, which is connected to guanine di-phosphate (GDP) receive a further phosphate, the product of the phosphorylation is guanosine tri-phosphate (GTP). (69, 70) Activated Ras together with Raf phosphorylates MEK, this leads to ERK phosphorylation and to activation of ELK, that enters into the nucleus and leads to the translation of the protein fos. (69, 70) Fos is one part of the heterodimeric transcription factor AP1, whose second part is the phosphorylated Jun. (69, 70) The activation of Jun, is also due to Ras MAPkinase pathway (JNK instead of ERK). (11, 69, 70)

The second and third pathways are connected through PLCγ1, a protein which is also recruited to LAT and is phosphorylated by ZAP70 and Itk. (69, 70) PLCγ1 hydrolyses the phosphatidylinositol-2-phosphate (PIP_2) to inositol 3 phosphate (IP_3) and Diacylglycerol (DAG). (11, 69, 70) IP_3 leads to an increase of cytosolic calcium (Ca^{2+})-ions, due to the opening of the Ca^{2+}-channels in the smooth ER and in the cytoplasma membrane. (69, 70) The increasing amount of Ca^{2+} leads to recruitment of the heterodimeric calmodulin and calcineurin. (69, 70) These complexes activate cytoplasmic nuclear factor of activating T cells (NFAT). (11, 69, 70) DAG accumulates in the plasmamembrane and recruits PKC. (11) PKC

has an influence on decomposition of the inactive heterotrimer NFκB to the active heterodimer that is able to enter into the nucleus. (11, 69, 70)

The transcription factor complex comprised of NFκB (heterodimer), NFAT and AP1 activates the transcription of IL-2 mRNA. (69, 70) The IL-2 transcription is initiated by activating signal of the APC. Moreover, upon activation the IL-2 receptor α-chain (CD25) is de novo expressed. This contributes to the formation of the high affinity receptor ($K_D=10^{-11}$). (67, 71-74) The IL-2 receptor adapts to a trimeric conformation during the binding of IL-2. (67) This interaction leads to sustained proliferation and survival of T cells. (67, 72, 73) The first step in IL-2 signalling is the phosphorylation of the intracellular domains of the β-chain (CD122) and γ-chain (CD132). (67, 75) Several kinases are phosphorylated and implicated in IL-2 induced signalling, which subsequently leads to gene expression and multi-effector function. The implicated signalling proteins are Syc, Src and STAT. (67, 76) Syk and Src are withheld from CD122. (67) STAT is activated by the CD132 intracellular domain. (67, 77, 78)

The strong IL-2 dependence of T cells ($CD4^+$) after activation, which includes a high affinity binding, let us to speculate whether it would be possible to detect such T cells by IL-2 decorated VLP. For that purpose we fused the IL-2 gene to the GPI-anchor of CD16b and we generated fluorescent VLP (FS). IL-2::GPI decorated FS would allow in this way the detection of activated, proliferating T cells.

1.5 Interleukin-2 receptor

The IL-2 receptor consists of three chains, the α-chain (CD25), the β-chain (CD122) and the γ-chain (CD132) (67) The β- and γ-chain are constitutively expressed on resting lymphocytes. (67) This heterodimeric receptor acts as the intermediate receptor, with an affinity of $K_D=10^{-9}$ M. (67) CD25 has an affinity of $K_D=10^{-8}$M, and is not expressed in resting T cells. (67, 79) The complete receptor corresponds to the high affinity receptor with $K_D=10^{-11}$M, which is expressed on activated T cells. (67)

1.5.1 The α-chain (CD25) and its promoter

The α-chain (CD25) molecule is a type I transmembrane protein, which contains 219 extracellular and 13 intracellular aa. (67) CD25 is localized on chromosome 10p14-15, the receptor is composed of eight exons and seven introns. (67, 80-82) The induction of the expression happens quickly after antigen recognition. (67, 83-86) The promotor region of CD25 is composed of three positive regulatory regions (PRR) I-III. PRR I reveals a very complex binding domain, which requires several transcription factors. (67) PRR I contains binding regions for NFκB, serum responsive factor (SRF) and Sp1. (67) Furthermore, there are two factors binding upstream of NFκB also in, NFIL-2RA or UE1. (67, 87, 88) Downstream of PRR I, is PRR II localized which binds Elf-1 (Ets family protein) and the high mobility protein HMG-I(Y). (67, 89) PRRIII is localized upstream of PRRI and possesses own binding domains for Stat5, Elf-1 and GATA-1-like protein. (67) PRRIII and PRRII are essential for IL-2 mediated α- chain (CD25) promoter. (67) It is expected, that these two promoter regions require functional cooperativity. (67)

1.5.2 The β-chain (CD122) and its promoter

The β-chain (CD122) is also a type I transmembrane consisting of 214 aa in the extracellular and 286 aa in the intracellular domain. (67) The β-chain is localized on chromosome 22q11.2-12 and is composed of 10 exons and nine introns. (67, 90, 91) The CD122 is expressed already in resting T cells (67, 79, 92) The promoter region of CD122 contains three enhancer-like regions. (67, 93) The first like enhancer region binds GABP and the Ets family proteins Ets-1 and the second region recruits the Sp1 factor and early gene product Erg-1. (67, 93, 94) The third region contains negative regulatory elements (NRE). (67, 93)

1.5.3 The γ-chain (CD132) and its promoter

The γ-chain (CD132) has 232 extracellular aa and 86 intracellular aa and is a type I membrane protein, located on the X–chromosome. (67) The gene is organized in eight exons and seven introns. (67, 95-97) CD132 is constitutively expressed (67,

77, 78) and contains an enhancer binding domain for Ets that mediates the activity. (67, 98)

The diverse affinities of the IL-2 receptor lead us to test the hypothesis, whether it would be possible to distinguish these differences by binding of FS decorated with IL-2::GPI. This was the reason for the creation of IL-2 receptor-components which are GPI-anchored. The components can be tested in different combinations with IL-2::GPI FS on transfected HEK-293 cells. Another possibility is the opposite situation, by staining of IL-2::GPI decorated HEK-293 with IL-2 receptor chain-combinations decorating FS.

1.5.4 Consequence of Interleukin-2 receptor chain knock-out

The loss of the interleukin receptor chains leads to severe combined immunodeficiency (SCID). Patients suffer from lack of adaptive immune cells, and therefore they are not capable to generate neither specific T cell dependent antibody responses nor cell-mediated responses. (69, 70) Furthermore, the capability of developing immunological memory is severely compromised. (69, 70) A severe form of SCID is the X-lined SCID, which is frequently caused by the loss of the common γ-chain (CD132). (69, 70) CD132 is the signal transducing element for several interleukins, among them IL-2, IL-4, IL-7, IL-9 and IL-15. (99-107)

Affinity	Composition	Kd	Cellular distribution
Low	α-chain (CD25)	10^{-8}M	Not expressed in resting T cells
Inter-mediate	β-chain (CD122) and γ-chain (CD132)	10^{-9}M	Resting lymphocytes, especially NK-cells
High	α-chain (CD25), β-chain (CD122) and γ-chain (CD132) IL-2R	10^{-11}M	Activated lymphocytes

Table 1. The IL-2 receptor chain affinities. (67)

A consequence of α-chain mutations or knock-out of CD25 is incomplete T cell development. (69, 70) The loss of CD122 leads to increased autoimmunity. (69, 70) Loss of both chains CD122 and CD132 causes severe immunodeficiency. (69, 70)

Chains	Extra-cellular	Trans-membrane	Intra-cellular	Molecular weight
α-chain (CD25)	219 aa	19 aa	13 aa	55-60 kDa
β-chain (CD122)	214 aa	25 aa	286 aa	~75 kDa
γ-chain (CD132)	232 aa	29 aa	86 aa	~65 kDa

Table 2. The structure of the original human IL-2 receptor chains with the length of the each domain in amino acid (aa) and the corresponding molecular weight. (67, 72, 75, 77)

1.6 Interleukin-7 function

Interleukin-7 (IL-7) was initially described as 25 kDa factor having activating effects on B cells. (107, 111). Afterwards, it was discovered that it has also an activating and proliferation inducing influence on T cells. (99, 112-114) The importance of IL-7 for the development of T and B cells was proven by depletion of IL-7 or by α-chain (CD127) knock-out of IL-7 receptor in mice. (99, 107, 115) IL-7 deficient mice, (99, 109, 110) lack T cells, B cells, NK cells, NKT cells, whereas CD127 deficient mice show a more severe phenotype (108-110) These experiments show the necessity for IL-7 for both T and B cells, demonstrating that IL-7 is a critical factor during lymphopoiesis. (107) IL-7 expression was detected in primary and secondary lymphatic organs such the thymus, bone marrow, spleen, and fetal liver. (107, 116-120)

Primary producers of IL-7 are fibroblastic reticular cells in lymph nodes in the T-cell zone (108, 121) The IL-7 receptor binds IL-7, via its heterodimeric components, (108, 122) which is composed of the common γ-chain (CD132) and the IL-7 α-chain (CD127). (101, 103, 107, 108, 122-124) In general IL-7 provides pro-survival and proliferating signals which directly influence T and B cell development and homeostasis. (108, 125) IL-7 receptor signalling is linked to the Jak-Stat and PI3K-Akt pathways. (108, 126) The consequence of the activation of

these pathways by IL-7 results in differentiation, survival and proliferation. (108) The IL-7 dependence of T and B cells initiated us to study the IL-7 expression on this cell types by our FS decorated with IL-7::GPI.

1.7 The green fluorescent protein

The Green fluorescent protein (GFP) is a naturally existing molecule and originates from *Aequorea victoria* of the Cnidaria Family. (4, 5, 127) Since, the cloning (Chalfie et al., 1994) of the wild type (wt) GFP, improved versions of the molecule have been engineered. They cover a brighter spectral range, exhibit enhanced photostability, have a reduced oligomerization tendency and are pH insensitive. (127) The new spectral range of the modified wt GFP contains different colors for example, blue (BFP), cyan (CFP) and yellow (YFP) (Heim et al., 1994; Ormö et al., 1996; Tsien, 1998). (127)

The molecular structure of GFP (Fig.5), is a 40 Amströng (Å) high and 30 Å broad β-barrel architecture. (127) The β-barrel of GFP is composed of 11 β-sheets and four α-helices. (127) The emission spectrum of GFP ranges from 500 nm to 525 nm, this wavelength can be modified by mutation of different regions in the protein. (127) Another recently discovered fluorescent protein is mcherry of *Discosoma sp.* (4-6), which was chosen for the creation of a deep red (cherry) emitting light at a wavelength of 630 nm to 660 nm and which we applied for FS utilized for double staining.

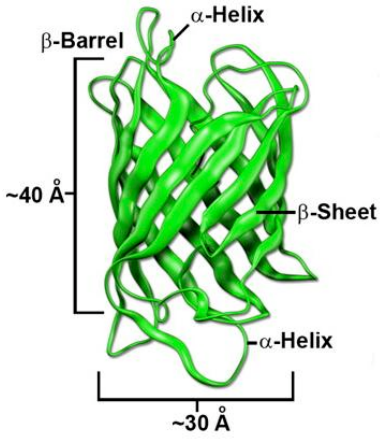

Figure 5. Structure of the green fluorescent molecule (GFP)
from: Nathan C. Shaner, George H. Patterson and Michael W. Davidson (2007) Journal of Cell Science 120, 4247-4260

1.8 Induction of fluorosome production

The research based on the use of virus-like particles (VLP) as platform to immunomodulate the function of T-lymphocytes is well established in our laboratory. In this project we aimed at engineering a novel staining tool, based on the VLP system platform i.e. fluorosomes (FS). This newly engineered staining tool, should allow identification of target cells, expressing receptors or interleukins (Fig.6).

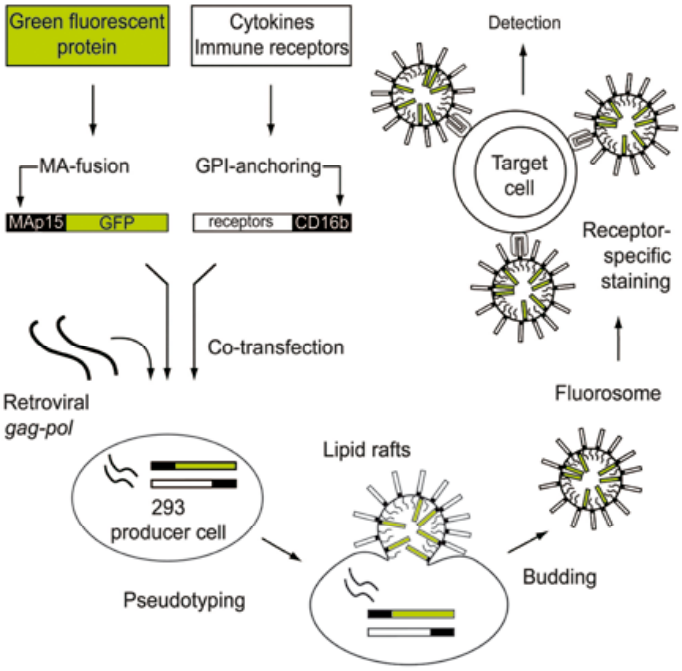

Figure 6. Production scheme of fluorosomes (FS) in MA::GFP stable HEK-293 cells.

The induction of FS budding is dependent on three components (Fig.7). The first component is the original gag/pol (OGP) from MoMLV. The gag/pol (OGP) leads to induction of VLP. (1, 2) The second component is the MA::GFP, which is composed of the GFP fused to the matrix protein (MA) p15 from MoMLV. The third component can be the interleukins or interleukin receptor-components, which are coupled through a glycine-linker to the GPI-anchor of CD16b. FS were variably decorated with the following constructs: IL-2::GPI, IL-2::GPI receptor-components (CD25::GPI,CD122-GPI and CD132::GPI) and IL-7::GPI. Constructs were chosen because of technical reasons but also because of their involvement in important immunologic processes. Current limitations of our system are the types of

transmembrane protein classes which allow only the use of type I membrane proteins. Both, the MA and the CD16b are molecules, which are targeted into the lipid rafts. The MA molecule attaches to the inner leaflet, the CD16b molecule to the outer leaflet of the plasma membrane.

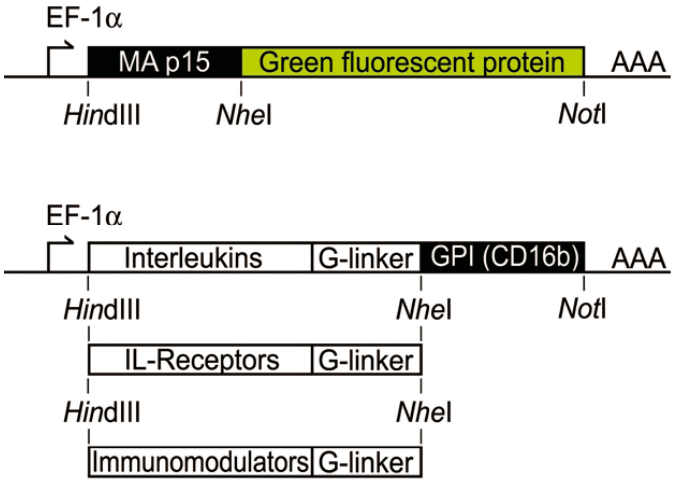

Figure 7. Raft targeted constructs MA::GPF and GPI- anchored IL or IL-receptor.

2 Materials and Methods

2.1 Expression constructs

The human IL-2 specific cDNA sequence was amplified with primers IL-2 for 5´-CGCGGGAAGCTTGCCACCATGTACAGGATG-CAACTCCTG-3´, IL-2 rev 5´-CCCGCGGCTAGCGCCGCCGCCAGTCAGTGTTGAGATGATGC-3` from clone pTCGF-11 (ATCC #39673, American Type Culture Collection, Manassas, VA), derived from PHA activated peripheral blood cells.

The 5´- ends of the cytokine cDNA were optimized for translation initiation by inserting GCC ACC in front of ATG. Hind III and Nhe I restriction sites were inserted. The naturally occurring stop codon was deleted by exclusion via PCR. Restriction with the corresponding enzymes allowed fusion of the fragment with the GPI-anchor acceptor sequence of CD16b. The original MoMLV gag/pol (OGP) was expressed using the mammalian expression vector pMD.gag/pol kindly provided by Dr.R. Mulligan, Boston, MA. The human CD16b served as negative control in the experiments.

Primer	Sequence	RE sites
GFP	for 5'-CCCGCGGCTAGCGTGAGCAAGGGCGAGGAG-3'	Nhe I
GFP	rev 5'-GCGCCCGCGGCCGCTTTACTTGTACAGCTCGTCCATG-3'	Not I
IL-2	for 5'-CGCGGGAAGCTTGCCACCATGTACAGGATG-CAACTCCTG-3'	Hind III
IL-2	rev 5'-CCCGCGGCTAGCGCCGCCGCCAGTCAGTGTTGAGATGATGC-3'	Nhe I
IL-2Rα	for 5'-CGCGGGAAGCTTGCCACCATGGATTCATACCTGCTGATGTGGGGA-3'	Hind III
IL-2Rα	rev 5'-CCCGCGGCTAGCGCCGCCGCCCTGGTACTCTGTTGTAAATATG-3'	Nhe I
IL-2Rβ	for 5'-CGCGGGAAGCTTGCCACCATGGCGGCCCCTGCTCTGTC-3'	Hind III
IL-2Rβ	rev 5'-CCCGCGGCTAGCGCCGCCGCCGGTGTCCTTCCCAAG-3'	Nhe I
IL-2Rγ	for 5'-CGCGGGAAGCTTGCCACCATGTTGAAGCCATCATTACCATTCACATCCCTC-3'	Hind III
IL-2Rγ	rev 5'-CCCGCGGCTAGCGCCGCCGCCATTCTCTTTTGAAGTATTGCTCC-3'	Nhe I
IL-7	for 5'-CGCGGGAAGCTTGCCACCATGTTCCATGTTTCTTTTAGG-3'	Hind III
IL-7	rev 5'-CCCGCGGCTAGCGCCGCCGCCGTGTTCTTTAGTGCCCATC-3'	Nhe I
MLV MA	for 5'-CGCGGGAAGCTTGCCACCATGGGCCAGACTGTTACCACT-3'	Hind III
MLV MA	rev 5'-GCGCCCGCTAGCGGATCGAGGCGGGGTCG-3'	Nhe I

Table 3. List of primers used. The underlined regions indicate the restriction enzyme sites.

The MA::GFP was generated by using the p15 matrix protein of MoMLV (pMD.gag/pol) as PCR template for the membrane anchor. The primers were tailed with Nhe I and Not I restriction sites which allowed insertion into pEAK12 expression vector. These fragments were digested accordingly and were ligated into the pEAK12 expression plasmid.

2.2 Transformation of *Escherichia coli* MC1061

Plasmids were transformed into *Escherichia coli* (MC1061) using high efficiency heat shock transformation. Competent MC1061, which were mainly used in our laboratory for transformations, were stored in aliquots at – 80 °C. The aliquot were melted on 4 °C, for each transformation 100 µl from the MC1061 aliquot were transferred into a precooled 1,5 ml tube. Ligated plasmid DNA (1 µg) was mixed with competent bacteria by gently pipeting up and down. The mixture was incubated for 20 minutes at 4 °C. The competent MC1061 were afterwards heat shocked by incubating for 5 minutes at 37 °C. The heat shocked and transformed MC1061 were spread on selective plates containing 100 µg/ml ampicillin with glass beads. The pEAK12 vector carries an ampicillin resistance gene allowing selection of plasmid containing bacteria. The selective plates were covered with a layer of top agar, which was required for the regeneration of the transformed MC1061 and didn`t contain ampicillin. The plate was incubated overnight (16-18 hours) at 37 °C. Selected colonies were transferred into 4 ml selective LB broth with 100 µg/ml ampicillin and further incubated at 37 °C by shaking overnight.

LB medium:
20 g LB Broth Base (Gibco-BRL)
0,09 M NaCl
ddH_2O to 1 liter

2.3 Plasmid Mini-preparation

Preparation of DNA was achieved by using DNA purification kit (Nucleospin Plasmid) according to manufacturer's protocol. Single cell cultures, which were grown overnight in selective LB broth, were collected in 1,5 ml tubes and centrifuged at 11000 g (12.000 rpm) for 30 seconds at room temperature (RT).

The supernatant was removed and the cell pellet was resuspended in 250 µl buffer A1. The cell lysation step required 250 µl of buffer A2. The tube had to be inverted gently for ideal cell lysation. Addition of 300 µl buffer A3 represented the neutralization step, which stopped the lysation. The cell lysate was centrifuged for 10 minutes (11000 g; RT). Insoluble cell components were accumulated to a pellet. The clear supernatant, which contains the solved plasmid DNA, was completely transferred onto a silica membrane column (Nucleospin Plasmid). The column was placed into a 2 ml collecting tube and was centrifuged for 1 minute (11000 g; RT). The content of the collecting tube was discarded. In order to wash the silica membrane, the column was loaded with 600 µl of washing buffer A4. The column containing buffer A4 was once centrifuged for 1 minute (11000 g; RT). The column was then dried through centrifugation for 2 minutes, before the DNA was eluated. The collecting tube was discarded and column is transferred onto a 1,5 ml tube. The eluation was performed by the addition of 50 µl of buffer AE onto the column and centrifugation for 1 minute (11000 g; RT).

2.4 Plasmid Maxi-preparation

The plasmid maxi-preparation allowed the extraction of high quantities of plasmid DNA. The maxi-preparation required 1 liter of selective LB broth (100 µg/ml ampicillin). The transformed bacteria were grown over night at 37 °C. The bacteria were first centrifuged and pelleted in a RC-3C Sorvall tube at 10000 g (4200 rpm) for 20 minutes at 4 °C. After discarding the supernatant the bacterial pellet was resuspended by shaking in 40 ml of precooled solution I (10 mM EDTA, pH8). 80 ml of solution II (0,1 M NaOH; 1% SDS) were added to the solved pellet. The bacteria were lysed by gently swirling of the tubes and by incubating for 2 minutes, but not longer than 5 minutes. In a third step was added 40 ml of neutralization solution III (5M KOAc (pH4,7)), which stopped the lysation reaction. The resulting mixture was shaked vigorously.

The insoluble debris was removed through centrifugation at 10000 g for 10 minutes at 4 °C. The soluble supernatant containing the plasmid DNA was transferred into 250 ml tubes through a filter cloth. The tubes were filled with isopropanol and centrifuged at 10000 g for 15 minutes at 4°C. The supernatant was removed and the precipitated DNA pellet was washed once with 70 % ethanol and was dried with Kim Wipes (Hakle-Kimberly Clark, Vienna, Austria). The dried

pellet was resuspended in 4 ml 10 M EDTA, transferred into Sarstedt 14 ml tubes and was mixed with 5,5 g CsCl (Invitrogen, Groning, Netherlands), 100 µl 1 % Triton X-100 and 500 µl ethidium bromide (10 mg/ml). The solved mixture was centrifuged at 10000 g (10.000 rpm) for 10 minutes at RT with a JS-13.1 rotor. The supernatant was filled into Beckman polyallomer quick-seal tubes and sealed for ultracentrifugation. The tubes were centrifuged over night at 100000 g (80.000 rpm) in an Optima TLX ultracentrifuge (Beckman, Polo Alto, CA). The ultracentrigtion step leaded to the formation of the CsCl gradient which separated the plasmid DNA from chromosomal DNA. The lower band corresponded to the plasmid DNA the upper band was the chromosomal DNA. The plasmid DNA band should be in an optimal preparation bigger than the chromosomal DNA. After ultracentrifugation Beckman tube was cut open, the lower band was collected in a 2 ml syringe due to aspiration. The plasmid DNA was transferred to a Sarstedt 14 ml tubes. The next step required 10 ml n-butanol of NaCl saturated to extract the ethidium bromide from the plasmid DNA. The upper n-butanol phase was removed after 10 minutes holding time. These steps were repeated until coloration of the plasmid DNA, changed to a clear solution. The ethidium bromide purified plasmid DNA was precipitated with 1 x volume of 1 M ammoniumacetat, mixed well and added 2 x volume of 96 % ethanol. The precipitated plasmid DNA was centrifuged for 10 minutes at 10000 g with JS-13.1 rotor. The plasmid DNA pellet was once washed with 70 % ethanol and dried with cotton swabs. The pellet was resuspended in 400 µl TE-buffer (10mM TrisHCl; 1mM EDTA).
The DNA concentration was determined by optical density (OD) measurements at 260 nm. In order to control plasmid DNA digestion with corresponding restriction enzymes was performed. The digested plasmid was separated in agarose gel (Biozym LE agarose) melt in TAE-buffer.

50 x TAE stock:
242 g Tris-Base
57,1 ml Acetic Acid
100 ml 0,5 M EDTA
ddH_2O to 1 liter

2.5 Cell lines

2.5.1 Human embryonic kidney-293 cell line

The human embryonic kidney cell line 293 (HEK-293) was maintained in Iscoves Modified Dulbeccos Medium (IMDM) (Sigma Chemicals, St. Louis, MO) plus 10 % FCS (Invitrogen, Carlsbad, CA) supplemented with 2 mM L-glutamine, 50 µM 2-mercaptoethanol and 15 µg/ ml gentamycin sulfate. The HEK-293 cells were embryonic kidney epithelial cells transformed by DNA of adenovirus type 5. (66) HEK- 293 cells grow as adherent monolayer on the culture dish at 37 °C and 5 % CO_2. When cell confluence was reached after three days, cells were first washed with 1 x PBS. The PBS was removed from the cells and afterwards treated with trypsin that detached the cells from the culture dish by proteolysing the adhesion molecules of the HEK-293 cells. The treatment with trypsin required 5 minutes incubation at 37 °C. The detached cells were washed in 15 ml IMDM for the trypsinic digestion stop. The pellet was resuspended and washed once in IMDM for removing completely the trypsin. The cells were after this last washing step resuspended than counted and replated.

2.5.2 Mouse T cell line HT-2

HT-2 (ATCC, CRL-1841) cells, which are non-adherent and were maintained in NCM medium (supplemented). The cells were cultivated in the presence of 100 U/ml human IL-2 (Peprotech, London, UK). HT-2 cells were subcultured every three days at 1 x 10^5 cells/ml.

NCM medium (supplemented) for primary mouse cells:

RPMI 1640 (PAA laboratories)
12,5 % FCS (Invitrogen)
1,25 % Sodium Pyruvate 100 mM (Gibco)
1,25 % Non-essential amino acids mix 100 x (Gibco)
1,25 % L-Glutamycin 200 mM (Gibco)
0,25 % 2-mercatoethanol 50 mM (Sigma)
Gentamycin sulfate 50 mg/ml (Sigma)

3 % HEPES buffer 1 M pH 7,3 (Gibco)

2.6 Primary cells

2.6.1 Peripheral blood mononuclear cells

Peripheral blood mononuclear cells (PBMC) were isolated from heparinized blood of healthy adult donors upon informed consent by standard density gradient centrifugation with Lymphoprep (Technoclon, Vienna, Austria). The isolation of cells was done by Ficoll method preparation. Ficoll also known as polydisperse mixtures of dextran, was used for separation of lymphocytes from erythrocytes. (128) The human whole blood was piled up carefully on the Ficoll and was centrifuged. The cells with high density like erythrocytes were collected at the bottom, the PBMC were collected in the upper part of the tube after the centrifugation. The PBMC could be recognized in the Ficoll, the respective cells looks like white clear coat that could be collected.
After isolation PBMC were maintained in IMDM or stored in fluid nitrogen with 2 x freezing medium. The cells could be activated via beads which resulted in cell proliferation. The activation was started 48 hours before using the cells as target in the staining experiments. The beads were coated with anti CD3/CD28 antibodies and were applied at a ratio of three beads per cell.

2 x freezing medium: IMDM, 20 % FCS and 10 % dimethyl sulfoxide (DMSO).

2.6.2 Peripheral blood mononuclear cells from chronic lymphatic leukemia patients

Whole blood samples of CLL patients obtained upon informed consent were anti-coagulated by EDTA and used in standard whole blood staining using LYSE-solution according to the manufacturer´s, recommendations (An der Grub, Kaumberg, Austria).

2.7 Ca_2PO_4-transfection of human embryonic kidney – 293 cells

One day prior to transfection HEK-293 cells were seeded in a 100 mm culture dish at a concentration of 3 x 10^6 cell/10 ml in IMDM containing 2,5 µg/µl plasmocin

(InvivoGen) and 1 µg/ml amphothericin (PAA). The medium was replaced at least half an hour before transfection with IMDM containing only 1 µg/ml amphothericin. Cells were covered with 2 ml transfection mix. The mixture was composed of 870 µl steril ddH_2O, 30 µg DNA, 100 µl $CaCl_2$ (2,5 M) and 1 ml 2 x HBS-buffer. After 18-24 hours transfection medium was replaced again and transfectant were cultured for a further 48 hours with IMDM containing 2,5 µg/µl plasmocin and 1 µg/ml amphothericin.

2x HBS (HEPES buffer saline):

NaCl (140 mM),
Na_2HPO_4 (1,5 mM),
HEPES (50 mM)
ddH_2O to 1 liter

	pEAK12 CD16::GPI	pEAK12 CD25::GPI	pEAK12 CD122::GPI	pEAK12 CD132::GPI
Intermediate Receptor	10 µg DNA	---	10 µg DNA	10 µg DNA
High-Affinity Receptor	---	10 µg DNA	10 µg DNA	10 µg DNA

Table 5. The DNA mix for HEK293 cell Receptor-components transfection.

	pEAK12 CD16::GPI	pEAK12 CD25::GPI	pEAK12 CD122::GPI	pEAK12 CD132::GPI	pMD gag/pol
Low-Affinity Receptor FS		7,5 µg DNA	---	---	7,5 µg DNA
Intermediate Receptor FS	7,5 µg DNA	---	7,5 µg DNA	7,5 µg DNA	7,5 µg DNA
High-Affinity Receptor FS	---	7,5 µg DNA	7,5 µg DNA	7,5 µg DNA	7,5 µg DNA

Table 6. The DNA mix for the optimal production of fluorosomes (FS) decorated with receptor-components.

	pEAK12 IL-2::GPI	pEAK12 IL-7::GPI	pMD gag/pol
IL-2::GPI_FS	22,5 µg DNA	---	7,5 µg DNA
IL-7::GPI_FS	---	22,5 µg DNA	7,5 µg DNA

Table 7. The DNA mix for the optimal production of FS decorated with interleukins.

2.8 Establishment of stably transfected human embryonic kidney-293 cells

Stable transfectants of HEK-293 cells with MA::GFP, GFP or MA::mCherry were generated by linearizing pEAK12 with the restrictions enzyme *Sfi I* (New England Biolabs) followed by transfection into HEK-293 cells by the calcium phosphate precipitation method. The transfectants were selected with puromycin 1 µg/ml (Sigma Chemicals) that was added to the IMDM.

The p_mCherry was cut with *Sfi I* (New England Biolabs), HEK-293 cells were transfected by the modified calcium phosphate precipitation method and selected by limiting dilution in 96-well flat bottom plates and maintained in IMDM.

Subcloned transfectants were analyzed by flow cytometry on a FACS Calibur (Becton Dickson, Palo Alto, CA) using the Cell Quest software.

2.9 Biochemical analyses

2.9.1 Cell lysis for Western blot analyses

The biochemical analyses of transfected cells required cell-lysates which were analyzed by Western blotting. The transfected cells were first of all removed from the plate with 0,5 mM EDTA/PBS and washed once with PBS. The cell number was adjusted to 10 x 10^7 and lysed with 2 x NP-40 Lysis buffer, for 30 minutes strictly on ice (4 °C). The cell-lysates were afterwards centrifuged for 10 minutes at 80 g (1000 rpm) in an Eppendorf Centrifuge 5424. By this step insoluble cell components form a pellet and were removed. The supernatants were used for further analyses and 4 x reducing or non-reducing Laemmli sample buffer was added.

To perform Western blot with VLP preparations it was required to concentrate the secreted VLP in the crude supernatant by ultracentrifugation. The crude supernatant was therefore collected and filtered through 0,45 µm Filter (Sarstedt). The filtered supernatants were transferred to Beckman Centrifugation Tubes (Beckman Instruments, Inc.; Palo Alto, CA; USA) and ultracentrifuged at 100.000 g

(28.000 rpm) for 1 hour on Beckman-Optima LE-80 K centrifuge (Beckman) with SW-41Ti. The pellet was resuspended in 100 µl 1 x Laemmli sample buffer selective in reducing or non-reducing.

2.9.2 Isopycnic sucrose gradient centrifugation

The isopycnic sucrose gradient method separated the cell components due to their density, which was important for the detection of lipid raft targeting. The analyzed cells were therefore removed from the culture plate with 0,5 mM PBS/EDTA. The cell number required for this experiment was 2 x 10^8. The complete experiment was strictly performed on ice (4°C) which means that all materials used have to be pre-cooled so as not to solubilize the GPI-anchored proteins from the lipid rafts. The cells were after the detaching from the plate washed once with ice old PBS. The cell pellet was resusupended in 1 ml ice cold PBS. The resuspended pellet was portioned in two 1,5 ml tubes with Triton X-100 2 x Lysing buffer and incubated for 30 minutes on ice. The non-ionic detergent Triton X-100 is important because ions interact with lipid rafts and the GPI-anchor which result in release of the component from each other. (34) The cell lysates were afterwards transferred to a glass douncer (Wheaton; Millville NJ; USA) and were dounced for 10 times. The dounced lysates were cast in 1,5 ml tube. The insoluble cell components were removed by centrifugation for 1 minute at 140 g (2000 rpm) in a Eppendorf Centrifuge 5424. The supernatant was collected and mixed due to invertation with the same volume of 80 % sucrose in 4,5 ml Cryo Tubes Vials (Nunc) from 10 minutes on 4 °C. To perform the stacking of the sucrose gradient 1,6 ml of the 40 % sucrose mixture containing the cell lysate was transferred in polypren Beckman Centrifuge Tubes (Beckman Instruments, Inc.; Palo Alto, CA; USA). The next layer of 30 % sucrose was stacked to a volume of 1,6 ml over the 40 % mixture. The last layer contained 5 % sucrose and had a volume of 0,8 ml. The three different layers that can be distinguished by light reflection at their interphases. The sucrose gradient was ultracentrifuged at 200.000 g (44.000 rpm) with SW-60Ti (Beckman) rotor without acceleration and brake at 4 °C overnight. The ultracentrifugation led to separation of the cell components according to their density. The gradient is collected in nine fractions 400 µl each. The upper fractions number 2 and 3 contained the lipid raft. The lower fractions (6, 7, 8 and 9) contained non lipid raft proteins.

The fractions were mixed with 4 x Laemmli buffer, reduced or non-reduced. The detection was performed by Western blotting.

2 x Triton X-100 Lysis buffer:
2 % Triton X-100
0,5 mM EDTA
25 µg/ml aprotinin
25 µg/ml leupeptin
1 mM phenylmethylsulfonylfluorid (PMSF)
Solubilized in 936 µl MBS (25 mM MES [morpholineethanesulfonic acid],150 mM NaCl]

2.9.3 Western blot

Samples were boiled at 95 °C for 10 minutes and shortly vortexed for cutting the chromosomal DNA. The mix was loaded on a 14-20 % tris polyacryl amid gel (PAGE) (Anamed). The gel aperture (Hoefer Pharmacia BioTech, San Francisco CA, USA) was filled with 1 x Gel running buffer, the loaded gel was run at 150 Volt. The gel was transferred on a pre-cut and methanol activated PVDF membrane (PVDF-Immunobilone P, Millipore) or alternatively non methanol activated Pure Nitrocellulose Membrane (Transfer-Blot, Transfer Medium, BioRad) and four blotting sheets (Filter Paper, Blot adsorbant Filter Paper, BioRad) to a Blotting buffer soaked sandwich on the blotting aperture (Hoefer Scientific Instruments, San Francisco CA, USA). The blotting time corresponded to 1 hour at 30 Volt. The blotted PVDF membrane is removed from the blotting sandwich and blocked with blocking buffer for 1 hour. After the blocking primary antibody could be added and incubated for 2 hours. The membrane was washed 3 times for 5 minutes with Washing buffer (PBS; 1%Tween). The second antibody which is HRP conjugated was added and incubated for 1 hour. The membrane was afterwards washed 3 times for 5 minutes in Washing buffer and developed in the darkroom by individual exposing on X-ray film (BioMax XAR Film, Scientific Imaging Film, Kodak) after incubation for 1 minute in chemoluminiscence substrate (Western Lightning, Enhanced Chemiluminescence Substrate, Perkin Elmer).

2 x NP-40 Lysis buffer:
2 % NP-40
0,5 mM EDTA
20 µg/ml aprotinin
20 µg/ml leupeptin
1 mM phenylmethylsulfonylfluorid (PMSF)
Solubilized in 940 µl MBS (25 mM MES [morpholineethanesulfonic acid],150 mM NaCl]

4 x Laemmli sample buffer:
4 % sodium dodecyl sulfate (SDS)
10 % glycerol
Bromphenol blue (is added to give a dark blue color)
For reducing Laemmli add 10 % β-mercaptoetanol.

10 x PAGE-buffer:
0,25 M Tris base
2,5 M Glycine
ddH_2O to 1 liter

1 x Gel Running buffer:
1/10 dilution with ddH_2O and 5 ml 20% SDS.

1 x Blotting buffer:
15 % 10x PAGE-buffer
30 % methanol
ddH_2O to 1 liter

Blocking buffer:
10 % milk powder
1 ml Tween20 (BioRad)
PBS to 1 liter

Primary Antibody			
CD59	MEM-43/5	mouse	Exbio, Praha, Cech Republic
CD147	MEM-M6/6	mouse	Exbio, Praha, Cech Republic
IL-2	IL-2.1F10	mouse	Dr. Majdic, Inst. Immunol, Vienna Austria
GFP		rabbit	antibodies-online, Aachen, Germany
CD25	AF2438	mouse	R and D systems, Vienna, Austria
CD80	mem223	goat	Exobio, Praha, Cech Republic
P30 Gag	R187	rat	ATCC, Ratitan, NY
Secondary Antibody			
Mouse Ig	goat		HRP DAKO, Glostrup, Denmark
Rat Ig	rabbit		HRP DAKO, Glostrup, Denmark
Rabbit Ig	goat		HRP DAKO, Glostrup, Denmark

Table 8. Primary and secondary immunoblotting antibodies (HRP, horse radish peroxidase)

2.10 Detection of the transfectants by bifocal microscopy

Stable transfectants were seeded at density of 4 x 10^4 cells/cm^2 in a PeCon POC-R cell cultivation chamber and were grown overnight at 37 °C and 5 % CO_2. The adherent cells were afterwards analyzed by microscopy on an Axiovert 100 M confocal microscope using a 63x/1.40 oil immersion objective (Carl Zeiss, Göttingen, Germany).

2.11 Flow cytrometric analyses of cells

For the analyses by flow cytometry the cells were removed from the culture dish with 0,5 mM ETDA/PBS and once washed with PBS and are centrifuged (500 g (1700 rpm); 5 min.) The pellet was resuspended in ice cold (4 °C) FACS buffer and cells were ceased to a number of 5 x 10^6 cells/ml (200.000 cells/50 µl). The cell number was measured with a cell counter (Z2 Coulter Counter, Cell and Particle counter, Beckman Coulter).

The FS producer cells HEK-293 MA::GFP and HEK-293 GFP were measured in FACS, after the determination of the cell number. The negative cell reference was used for life gating with propidium iodide.

50 µl (200.000 cells) of the read out cells HEK-293, HT-2 or PBMC were added to a volume of 20 µl antibodies or 20 µl FS (concentration 1 µg/µl) in 5 ml FACS tube (BD Falcon). Cells, which were performed with antibodies, were incubated on ice (4 °C) and cells performed with FS were incubated at room temperature. Both antibodies and FS required 30 minutes incubation time in the dark. The cells were afterwards washed with FACS buffer, centrifuged at 4 °C (500 g; 5 min.) and were resuspended in 100 µl FACS buffer. In case of secondary antibody, cell pellet was resuspended in 50 µl FACS buffer and incubated with secondary antibody for 30 minutes. Cells were washed once with FACS buffer after the incubation time.

Primary Antibody				
CD3	S4.1	mouse	APC	Invitrogen (Caltag), Carlsbad, CA
CD19	SJ25-C1	mouse	APC	Invitrogen (Caltag), Carlsbad, CA
CD99	3B2/TA8	mouse	FITC	Caltag Laboratories, Burlingame, CA
CD59	MEM43	mouse	FITC	Exobio, Praha, Cech Republic
IL-2	IL-2.1F10	mouse		Dr. Majdic, Inst. Immunol, Vienna Austria
CD25	2A3	mouse	FITC	BD-Pharmingen, San Diego, CA
CD122	27302	mouse	FITC	RD, Minneapolis, MN
CD127	R34.4	mouse	PE	Beckman-Coulter (Immunotech), Fullerton, CA
CD132	TUGh4	mouse	PE	BD-Pharmingen, San Diego, CA
Combitest neg. con.	GCT_202		FITC /PE	An der Grub (ADG), Kaumberg, Austria
CIAP VIAP		mouse	FITC	Dr. Majdic, Inst. Immunol, Vienna, Austria
IL-2	MQ1-17H12	rat	PE	BD-Pharmingen, San Diego, CA
Secondary Antibody				
Mouse Ig		goat	OG	Invitrogen (Molecular Probes), Eugene, OR

Table 9. The used primary and secondary antibodies in flow cytometry. (PE, phycoerythrin; FITC, fluorescein isothiocyanate; APC, allo phycocyanine; OG, Oregon green)

Whole blood staining required also cell concentration determination with Zap-Oglobin which lysed the erythrocytes. The cell number was adjusted with FACS buffer and cells were incubated with 20 µl antibody or FS for 30 minutes at room temperature (RT) in 5 ml FACS tubes. Cells were treated with 100 µl LYSE solution (An der Grub (ADG), Kaumberg, Austria) and incubated for 10 minutes. Afterwards 5 ml FACS tube was filled with ddH_2O, once incubated for 10 minutes and centrifuged (500 g; 5 min).

FACS buffer: 0,5 % bovo serum albumin (BSA); 0,05 % (10 %) Acid N3

2.12 Phosphatidylinositol phospholipase C release

The Phosphatidylinositol phospholipase C (PI-PLC) from *Bacillus thuringiensis* releases GPI-anchored proteins treated cells were afterwards analyzed by flow cytometry. For this purpose cells were removed from culture plate due to 0,5 mM ETDA/PBS and once washed with PBS and centrifuged (500 g (1700 rpm); 5 min.). The pellet was resuspended in ice cold (4 °C) PBS with the cell number of 500.000/50 µl. 50 µl of adjusted cells were treated with PI-PLC and 50 µl are left untreated as control. PI-PLC treated cells received 0,1 U/ml PI-PLC. Treated and untreated cells were kept for 2 hours at 37 °C to reach an optimal result, it is indicated to shake the samples occasionally. PI-PLC became unspecific after 2 hours, therefore it was important not to exceed the incubation time. The treated cells should be washed once with PBS (500 g; 5 min.) to remove the PI-PLC from the sample. The pellet was resuspended in ice cold (4 °C) FACS buffer to a cell number of 500.000/50 µl, add to 20 µl of primary antibody in 5 ml FACS tubes and incubated for 30 minutes on ice (4 °C) in the dark. The washing step was performed: By filling of the 5 ml FACS tube with FACS buffer, centrifugation (500 g; 5 min.) and pellet resuspention in 100 µl FACS buffer.

2.13 Purification and application of fluorosomes

The crude supernatant of stable MA::GFP cells that were transfected could be harvested after 72 hours and cleared of cellular debris by filtration through 0.45 µm (Millipore, Billerica, MA). The standard quantity used in our laboratory to obtain high particle concentration is 60 ml supernatant (10 ml supernatant per culture dish). The filtrated fluorosomes (FS) were concentrated due to ultracentrifugation in a Beckman-Optima LE-80K centrifuge (Beckman) the used rotor was the SW41Ti, at 100.000 g (28.000 rpm) for 1 hour and washed once in 10 ml PBS per culture dish. The supernatant was once centrifuged for 1 hour the FS pellet was resuspended in 120 µl FACS buffer. The protein concentration was measured by a standard protein assay (Micro BCA, Pierce). The standard protein assay uses a bovine serum albumin (BSA) standard curve to determine the protein

concentration of the sample. The BSA concentrations used for the standard curve are 200 µg/ml, 40 µg/ml, 20 µg/ml, 10 µg/ml, 5 µg/ml, 2,5 µg/ml, 1 µg/ml and 0 µg/ml (blank). The FS were diluted 1/100 and the sample was distributed in 96 well and was measured after 2 hours incubation at 37°C. The measurement was performed by a Photometer (ThermoMax Kinetic Microplate Reader, MWG-Biotech) at 595 nm. The BSA standard curve led to a raw value for the FS protein concentration. The raw value was multiplied with 100 x which corresponded to the dilution factor. The multiplied value represented the stock solution of the FS after ultracentrifugation. The protein concentration factor from 60 ml crude supernatant to 120 µl ultracentrifuged stock was 500 x. The stock solution was applied at a concentration of 1 mg/ml in a volume 70 µl, which contained the cells and FS.

3 Results

3.1 MA::GFP is targeted to the producer cell plasma membrane

3.1.1 Detection by bifocal microscopy

In a first step we compared MA::GFP and GFP transfected HEK-293 cells for their fluorescence characteristics. Our principle hypothesis was that the influence of the matrix protein (MA) fused to GFP would enhance targeting of the construct into lipid rafts. The signal emitted by MA::GFP cells should be exclusively detected in a high amount in the plasma membrane, which should in the additional presence of a budding trigger result in the secretion of high intense fluorosomes (FS). For GFP, which is a cytosolic protein, we would expect an even distribution throughout the cell and no targeting to the cell membrane. In a first step we generated stable transfectants for GFP and MA::GFP, which would allow us to produce FS under controlled conditions independently of transfection efficiencies.

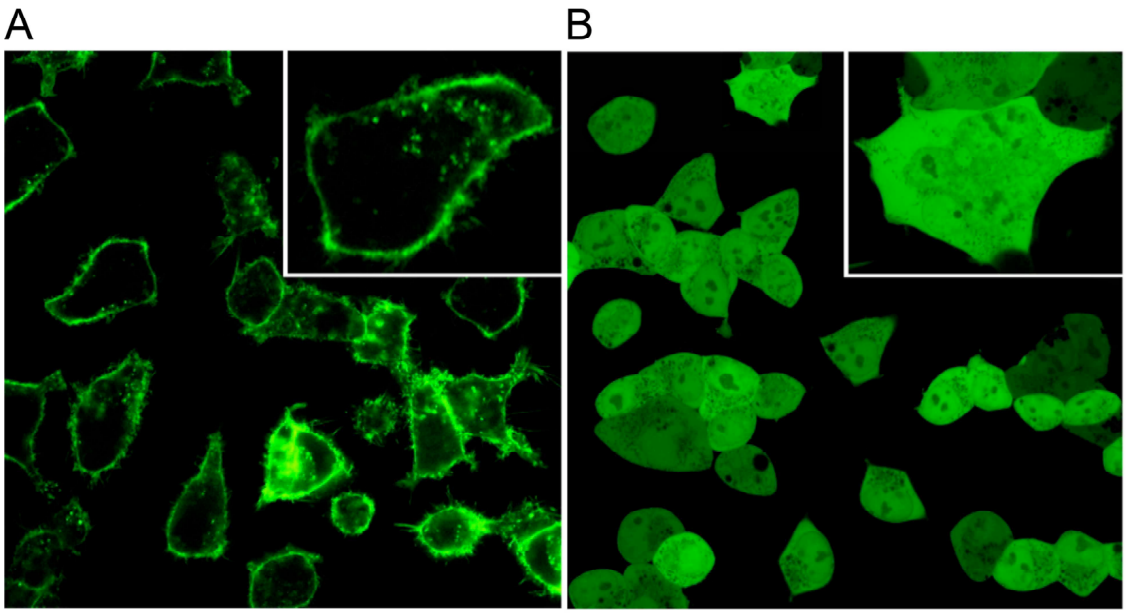

Figure 8. Microscopy picture of (A) MA::GFP and (B) GFP transfected HEK-293. Pictures (inset: high magnification) show characteristic morphology and fluorescence pattern.

The establishment of the stable HEK-293 MA::GFP and HEK-293 GFP, was achieved by linearization of pEAK12 vector containing the genes for MA::GFP and GFP. The vector was linearized with the *Sfi I* restriction enzyme. Successful integration of the construct was selected by culture in medium containing to

puromycin. In a first experiment GFP and MA::GFP expression levels and subcellular distribution were analyzed by confocal microscopy.

Figure 8A demonstrates the clear cut-association of MA::GFP with the membrane and gives already a first hint about fluorescence intensities. The soluble GFP expressed in the HEK-293 GFP stable transfectant (Fig. 8B) is distributed throughout the whole cell and is not concentrated in a special cell organelle or in the membrane.

3.1.2 Flow cytometric analyses of the producer fluorosomes cell

While targeting of the fluorescent dye is necessary for efficient fluorosomes (FS) production expression intensity also plays an important role. To clarify whether MA::GFP and GFP show fluorescence intensity in a comparable range we measured stable HEK-293 MA::GFP and stable HEK-293 GFP cells by flow cytometry to define mean fluorescent intensity (MFI) values of the corresponding transfectants.

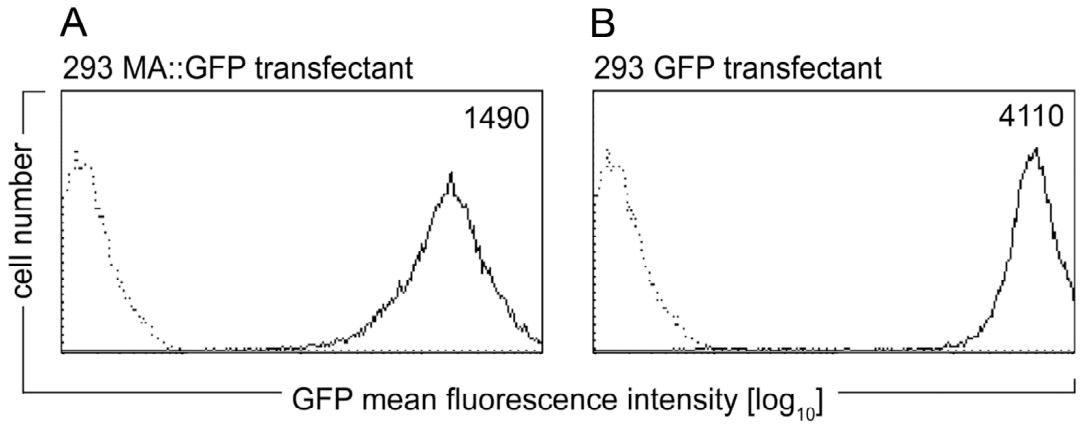

Figure 9. Flow cytometric measurement of the GFP expression intensity in fluorosomes (FS) producer cells. Overlay histograms of stable transfectant HEK-293 producer cells with (A) MA::GFP and (B) GFP (solid lines). The negative controls used for the overlay are wt HEK-293 cells (dotted lines). The values correspond to the reached mean fluorescence intensity (MFI) of MA::GFP and GFP transfectants respectively.

The flow cytometric results (Fig. 9) reveal that expression of MA::GFP in stable transfectants is in fact approximately 3-fold lower compared to intensity of GFP stable transfectants. The essential statement gained by these results, is that MA::GFP is preferentially targeted into the cell membrane and is strongly expressed in stable transfectants.

3.1.3 GFP fused to the matrix protein MA (MA::GFP) and Interleukin-2::GPI are targeted into lipid rafts

In order to take a more detailed look at lipid raft targeting we performed analyses of cell lysates after isopycnic sucrose gradient centrifugation.

For that purpose HEK-293 cells were transfected with IL-2::GPI, MoMLV gag/pol (OGP), MA::GFP or GFP and lysed. The lysis was strictly done at 4°C in Triton X-100. The method is based on separation of cell components via a sucrose gradient according to their density. Lipid rafts have a low density and are thereby separated from transmembrane components that have a high density. The lipid raft components can be found mainly in the second and the third fraction, while high density components especially transmembrane proteins are localized in the lower fractions 6, 7, 8 and 9.

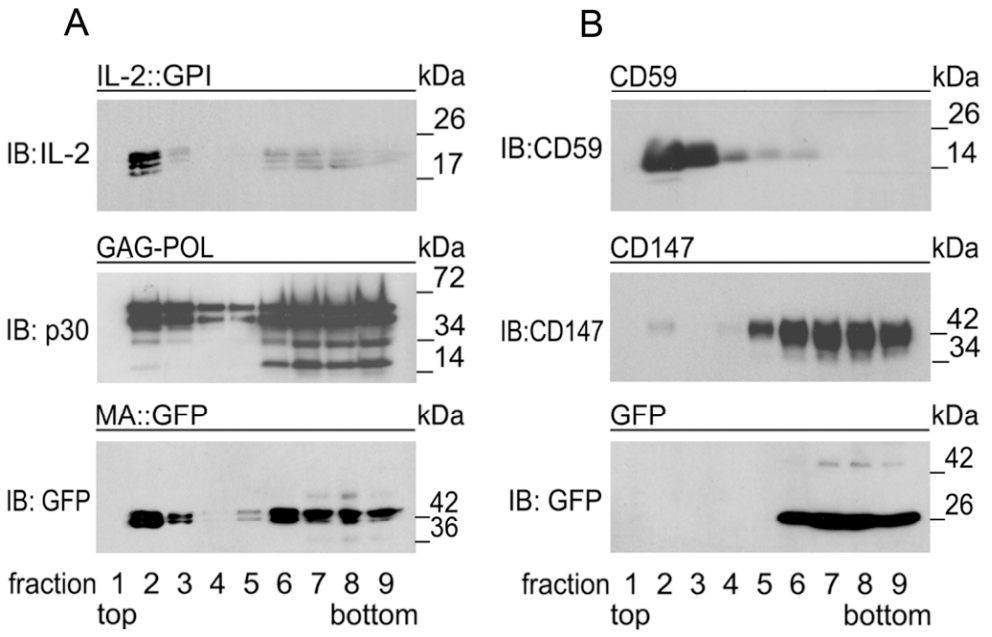

Figure 10. Isopycnic sucrose gradient of HEK-293 transfected with IL-2::GPI, MoMLV gag/pol (OGP) (p30Gag), MA::GFP and GFP. The blots in (A) correspond to cells transfected with hIL2, MoMLV gag/pol (OGP) (p30Gag) and MA::GFP, the blots in (B) correspond to lysates of transfectants probed with the indicated ingredients: hCD59 (pos. control), hCD147 (neg. control) and GFP (neg. control to MA::GFP).

The results of the sucrose gradients (Fig. 10) analyzed by Western blotting, confirm our expectations. All constructs used in the fluorosomes (FS) (IL-2::GPI, gag/pol (OGP), MA::GFP) are targeted to the lipid raft. The gradients demonstrate in all three cases strong signals in the second and third fraction. For IL-2::GPI (Fig.10A) we observed the clearest result with a strong signal in the second

fraction and only low signal in the fractions 6-9. The signal (Fig. 10A) of the capsid protein (gag/pol (OGP)) and MA::GFP are not clear-cut (Fig. 10B). Both gag/pol OGP) and MA::GFP show not only signals in the second and third fraction but also in the non lipid rafts fractions 6-9.

The used controls are CD59 and CD147. The CD59 (Fig. 10B) is a constitutively GPI-anchored molecule and used as positive control for sucrose gradients but also for PI-PLC releases. The CD147 molecule is a constitutively transmembrane protein, which is excluded from lipid rafts. The comparison of gag/pol (OGP) and MA::GFP with the negative controls CD147 and GFP, reveal for these two constructs also some signal in the upper fractions (2 and 3), while this was not the case for the negative controls. The negative controls, especially the GFP (Fig. 10B) transfectant don't show any signal in the upper fractions.

In conclusion, these analyses reveal that all three components are targeted well to lipid rafts at significant percentages and are therefore suited for the production of FS.

3.2 Comparison of fluorosomes from MA::GFP and GFP producer cells

3.2.1 MA::GFP fluorosomes show significantly stronger fluorescence intensity than GFP fluorosomes

The experiments described above show that MA::GFP is stronger targeted to lipid rafts and strongly expressed in stably transfected cells. The following experiments focus on the main question of our work, staining of target cells expressing a respective receptor with fluorosomes (FS).

As a proof of principle, we decided to compare the fluorescence intensity emitted from both particles, the MA::GFP$^+$ VLP (MA::GFP FS) and the GFP$^+$ VLP (GFP FS), on the HT-2 cell line. HT-2 is a mouse T cell line constitutively expressing the mIL-2 receptor on the cell surface, which also has the property to bind human IL-2. For that purpose, FS from the above mentioned MA::GFP and GFP stable transfectants were transiently transfected with human IL-2::GPI and gag/pol (OGP) of MoMLV to induce particle budding. These producer cells were cultured for three days, the secreted FS were purified from supernatants and were used for staining of the HT-2 cells as described in Material and Methods. FS were used in the same

way as antibodies, which means that the read out cells were incubated for 30 minutes at room temperature with IL-2::GPI decorated FS (IL-2::GPI FS), afterwards washed with FACS-buffer, centrifuged and analyzed by flow cytometry.
Furthermore, in parallel experiments we tried to block the mIL2-receptor by the addition of soluble IL-2. The aim of these inhibition experiments is to show the specificity of the binding reactions. For that purpose the HT-2 cells were pre-incubated for 30 minutes on ice with 5000 U soluble IL-2 and afterwards stained with human IL-2::GPI FS as described above.
Figure 11 (A) and (B) depict the staining with GFP FS and MA::GFP FS decorated with IL-2::GPI on the HT-2 readout cells. The staining results obtained with IL-2::GPI MA::GFP FS (Fig.11B) reached a geometric mean fluorescence intensity (geo MFI) of 467 compared to 26 for IL-2::GPI GPF FS. Thus IL-2::GPI MA::GFP FS revealed an approximately 20-fold stronger staining intensity compared to IL-2::GPI GFP FS. These results confirmed our hypothesis that the preferential targeting of MA::GFP into MA::GFP FS, results in high staining efficiency. In contrast, IL-2::GPI GFP FS, showed low staining intensities when using equal protein quantities and are thus not suitable for use in FS.
The results of the soluble IL-2 inhibition experiment (Fig. 11D), which represent an average of three independent experiments, reveal the specificity of binding reaction to the IL-2 receptor, of HT-2 cells. The first diagram of Figure 11D shows a standard staining with IL-2::GPI MA::GFP FS. This staining is our positive reference for the inhibition, which corresponds to 100% cell binding. The second diagram of Figure 11D corresponds to the inhibition experiment with soluble IL-2 and the third diagram shows the control-transfected cells, which is our negative control. As it can be recognized in the diagram one and two (Fig. 11D), soluble IL-2 blocks the IL-2 receptor of the pre-incubated HT-2 target cells. The consequence is the binding inhibition of IL-2 MA::GFP FS to the IL-2 receptor of HT-2 cells in a statistical significant manner. The soluble IL-2 inhibition experiment demonstrates the high binding specificity of the IL-2::GPI MA::GFP FS, while nearly 100% of the stained HT-2 cells lose their signal after incubation with soluble IL-2. Comparing the low reached binding percentage for both control-transfected FS and IL-2::GPI MA::GFP FS in the inhibition experiment determine a very high significance because of the less difference between both values.

The conclusion of the inhibition experiment with soluble IL-2 after pre-incubation of HT-2 cells is the confirmation of the specificity of the binding reactions which is completely inhibited subsequent binding of IL-2::GPI MA::GFP FS.

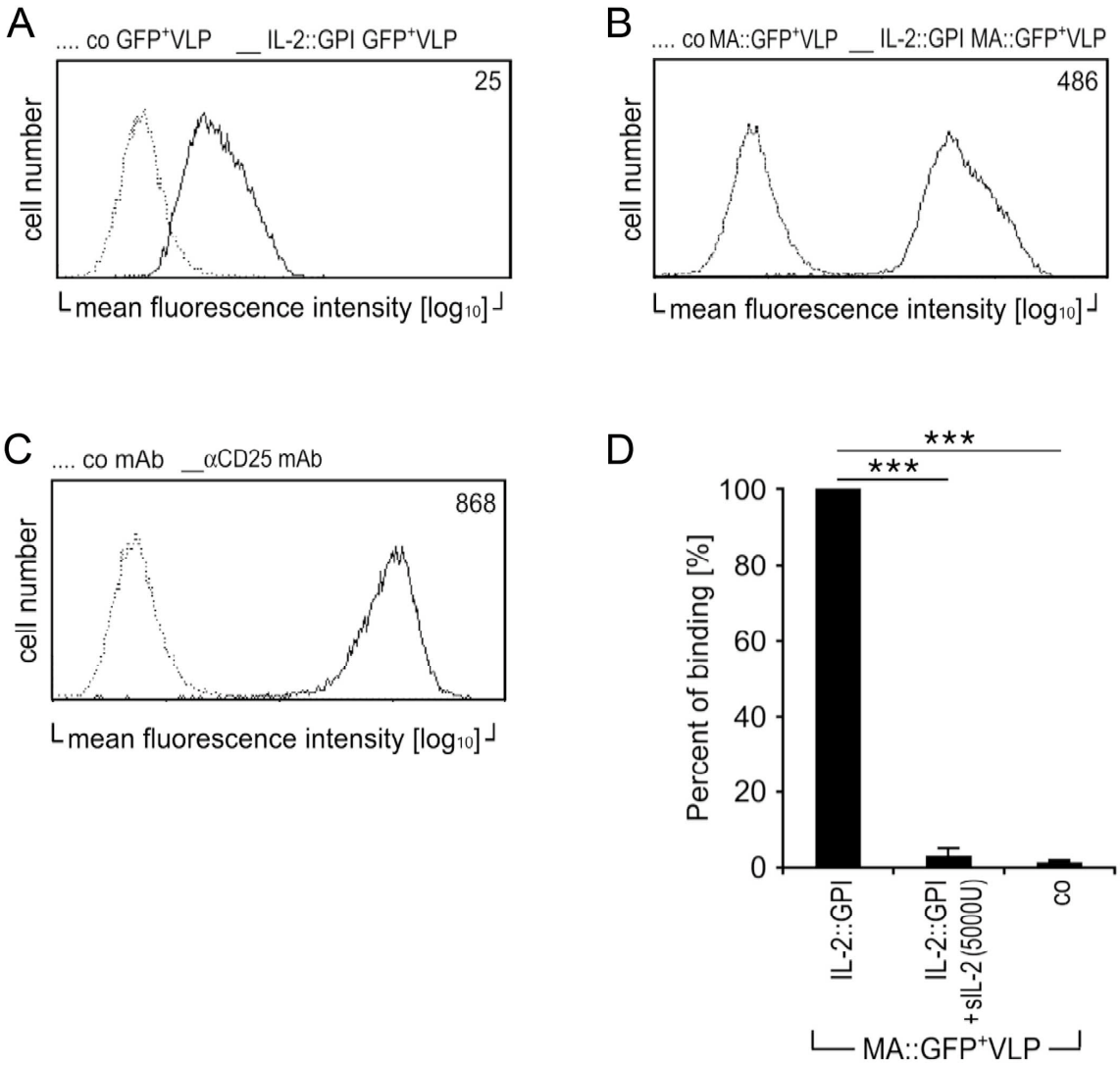

Figure 11. Overlay histograms of HT-2 cells (2 x 10^5) incubated with 30 µg IL-2::GPI MA::GFP$^+$ VLP (FS) or control MA::GFP$^+$ VLP (FS) (B), IL-2::GPI GFP$^+$ VLP or control GFP$^+$ VLP (FS) (A), and anti-CD25 mAb or control mAb (C) are shown. Specific fluorescence (solid lines) is compared to the respective control (dotted lines). Numbers indicate geo MFI values of specific reagents.
Exogenous IL-2 inhibits binding of IL-2::GPI MA::GFP$^+$ VLP (FS) (D). Native HT- 2 cells (2 x 10^5) or HT-2 cells pre-incubated with recombinant soluble human IL-2 (5 x 10^3 U) for 30 min. on ice were incubated with IL-2::GPI decorated MA::GFP$^+$ VLP (FS) and analyzed by flow cytometry. Results show binding of IL-2::GPI decorated MA::GFP$^+$ VLP (FS) to IL-2 pre-incubated relative to native HT-2 cells (mean + SD).

3.2.2 Western blot analyses of MA::GFP and GFP producer cells and their corresponding fluorosomes

Furthermore, we wanted to investigate the reason for the different staining intensities shown in Figure 11. Our hypothesis is that GFP fluorosomes (FS) contain decreased concentration of soluble GFP which is spread in the cytosol and is transfused into the particles during the secretion process from GFP stable transfectant. The reduced fluorescence intensity of VLP bearing soluble GFP compared to MA::GFP was confirmed by GFP-specific immunoblotting.

For that purpose, HEK-293 producer cells stably transfected with MA::GFP or GFP were transiently transfected with gag/pol (OGP) for the VLP induction and afterwards cultured for three days. Afterwards, cell lysates were prepared and the FS were collected from the supernatant and purified. These cell lysates and the purified FS were specifically immunoblotted for GFP and p30 Gag which was used as loading control.

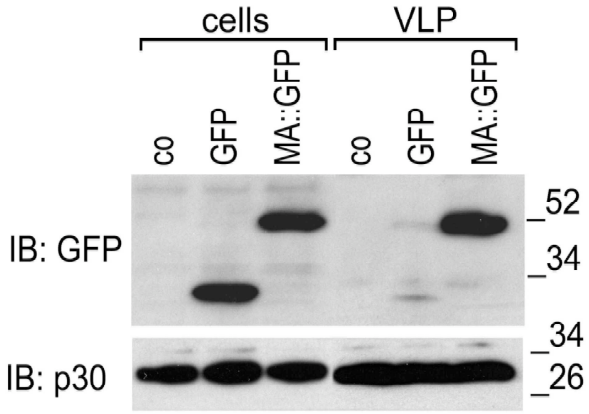

Figure 12. Differential targeting of MA::GFP and GFP to VLP (FS). HEK 293 cells were transfected with the indicated expression plasmids or control plasmid and cell lysates (cells) and corresponding VLP preparations were analyzed by SDS-PAGE under reducing conditions followed by immunoblotting (IB) with a GFP-specific goat antiserum or the p30 Gag (gag/pol (OGP)) specific mAb R187, respectively. Bound antibodies were detected by a HRP-conjugated secondary reagents and a luminol-based detection system.

The GFP specific immunoblotting (Fig. 12) for both MA::GFP and GFP producer cells reveal approximately the same signal intensity when using a comparable cell number. As expected the specific band for MA::GFP shows high molecular weight (~52 kDa) compared to GFP (~30 kDa), which is due to the fusion of the GFP gene to matrix protein (MA) more heavy. The control transfected cells don't show any signal. However, immunoblotting of the purified supernatant reveal different

signal intensities for GFP. In the MA::GFP FS probe, a strong bound can be found, while in the GFP FS only a weak residual GFP signal is detectable. As expected no signal is found in the control vesicle. Especially this experiment confirms the hypothesis of inefficient GFP targeting into GFP FS.

3.2.3 Dose-dependent quantification of binding of Interleukin-2 decorated MA::GFP and GFP fluorosomes to HT-2 cells

In the following experiment we addressed the question of dose dependent binding of fluorosomes (FS) to determine the ED_{50} for HT-2 binding. Therefore we tried both to determine the FS concentration needed to predict positively stained cells and staining intensities measured by the geometric mean fluorescence intensity (geo MFI) of the target cells. For that purpose, we analyzed the binding of titrated IL-2 decorated MA::GFP^+ VLP (IL-2::GPI MA::GFP FS), compared to IL-2 decorated GFP^+ VLP (IL-2::GPI GFP FS) by flow cytometry to HT-2 cells. The control-transfected CD16b MA::GFP^+ VLP (MA::GFP FS) and GFP^+ VLP (GFP FS) were also titrated as negative control, giving a hint about the background binding.

Figure 13A shows the FS titration of the IL-2::GPI MA::GFP FS which leads to a sigmoid curve with a saturating binding at 4 µg FS (>95% of HT-2 positive). We obtained a half maximal binding (ED_{50}) with 1 µg IL-2::GPI MA::GFP FS. The ED_{50} corresponds to 50 % of positive stained target cells reached with 1 µg using IL-2::GPI MA::GFP FS. In contrast the titration with IL-2::GPI GFP FS reaches the same value with almost 15 µg. In marked contrast, IL-2::GPI GFP FS produced significantly weaker signals, with only 62 % positive cells at the maximal concentration. The staining with both CD16b control-transfected FS reveals also that high particles quantities result in minimal background staining. The result of this titration experiment shows the particle quantities needed to reach a saturation point and a half maximal binding of IL-2::GPI MA::GFP FS and it underlines the quantitative difference of both FS preparations in staining of HT-2 cells.

Figure 13B shows the correlation between the quantity of FS used for staining and the corresponding geo MFI of the stained HT-2 cells. The staining intensity reached a geo MFI of 467 using 30 µg of IL-2::GPI MA::GFP FS, compared to 26 for IL-2::GPI GFP FS. Both, CD16b control–transfected FS (MA::GFP and GFP) show very decreased geo MFI < 8. The result of this experiment shows the

application of the FS as they give the quantitative evidence for the high staining efficiency of IL-2::GPI MA::GFP FS. Furthermore they allow to determine the optimal protein concentration for staining.

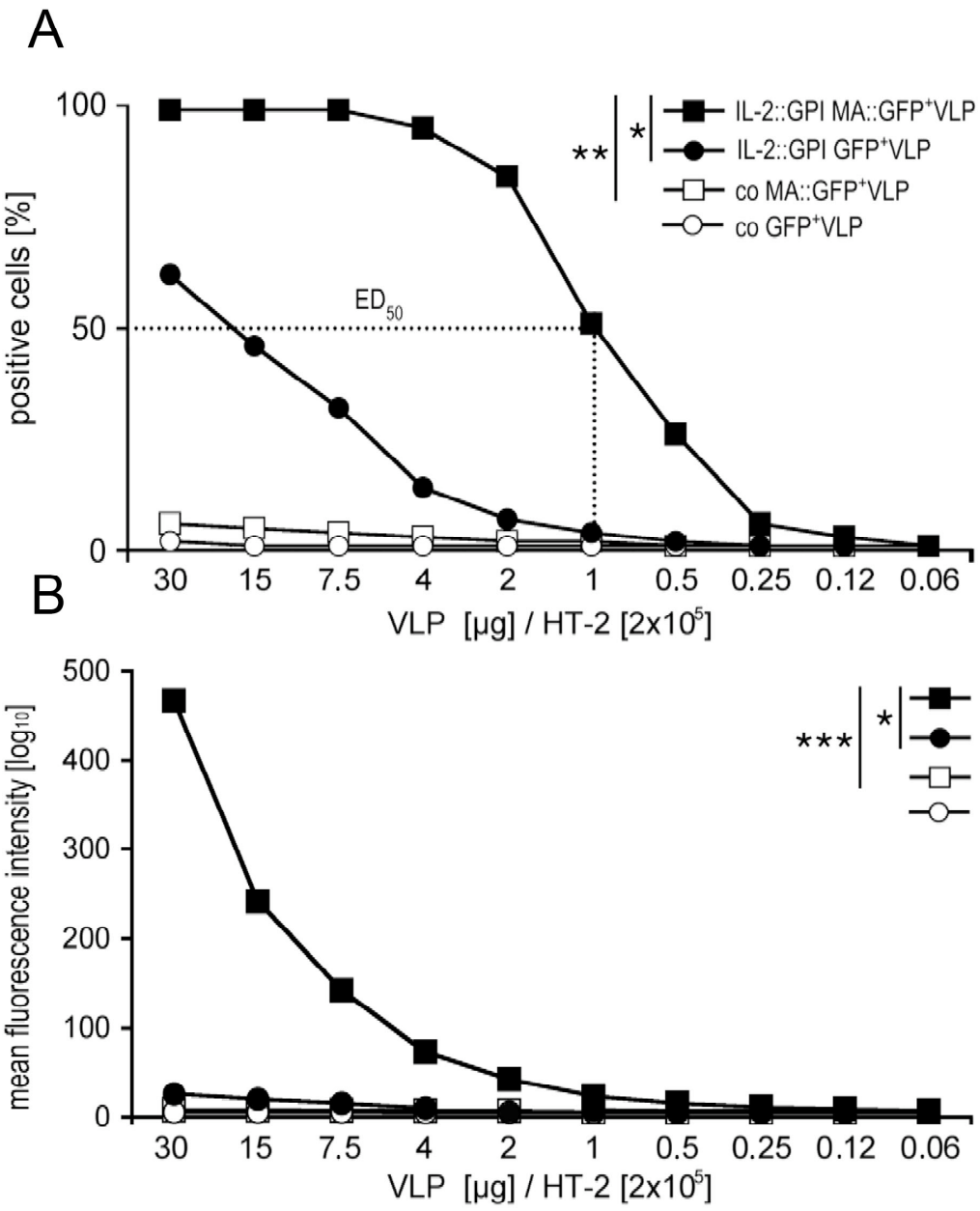

Figure 13. Binding of IL-2 decorated FS to IL-2 receptor positive HT-2 cells. Dose dependent binding. Two-fold dilutions of similar amounts of purified IL-2::GPI MA::GFP$^+$ VLP (FS) (closed squares), control MA::GFP$^+$ VLP (FS) (open squares), IL-2::GPI GFP$^+$ VLP (FS) (closed circles) and control GFP$^+$ VLP (FS) (open circles) were incubated with HT-2 cells (starting with 30 µg VLP / 2 x 10^5 HT-2 cells) at room temperature for 30 min, washed twice and analyzed by flow cytometry. (A) Percent positive cells and (B) geometric mean fluorescence intensities (geo MFI) obtained are plotted against the VLP concentrations applied. Native HT-2 cells revealed a geo MFI of 5 (< 2 % positive cells). ED50 is shown as dotted line. Statistical significance was calculated by the two-tailed Mann Whitney U-test; * $p < 0.05$; ** $p < 0.01$; *** $p < 0.001$

3.3 Evaluation of fluorosome stability

3.3.1 Fluorosome stability over time

We wanted to know more about the staining activity of our fluorosomes (FS) upon storage for different periods of time. This investigation of the FS stability was also performed on HT-2. The FS were tested for time and temperature stability. The stability criterion of the FS is very important. For all experiments described so far, freshly isolated and purified FS were used. However, in order to be able to apply the FS routinely we had to determine whether FS remain stable over prolong stronger times. For diagnostically application it is necessary to know, how to store the particle and how long.

As a proof of principle for the stability of IL-2::GPI MA::GFP FS upon prolonged storage at 4°C, five independent IL-2::GPI MA::GFP FS preparations were tested over the time length of four weeks. These FS preparations were once isolated, purified and used for the staining experiment. The remaining preparation was stored at 4°C and used to evaluate staining ability on HT-2 cells every week.

Sample	GeoMean (day 0)	GeoMean (day 7)	GeoMean (day 14)	GeoMean (day 21)	GeoMean (day 28)	GeoMean (Δ_{0-28} in %)[a]
VLP #1	115	119	124	122	68	40.9
VLP #2	108	108	111	112	62	42.6
VLP #3	135	148	146	121	85	37.0
VLP #4	112	110	116	120	63	43.7
VLP #5	98	98	92	72	44	55.1
Mean	113,6	116,6	117,8	107,4	64,4	43.9
SD	±13.6	±19.1	± 19.7	±21.3	±14.6	6.8

Table 10. Stability of IL-2 decorated fluorosomes upon prolonged storage at 4°C. Five particles samples measured independently of each other. First geometric mean fluorescence intensity (geo MFI) (day 0) is the reference value, following values are obtained by measurements every 7 days. The Mean corresponds to the average and SD is the corresponding standard deviation. Geo MFI [a] % variation compared to initial value (day 0).

The values (Tab.10) reveal that particle staining intensities stay unchanged for three weeks. After that time, FS rapidly lose staining capacity. The reason for this observation cloud be the complexity of our tool which is a whole virus containing a

broad range of different molecules such as capsid proteins, the decoration proteins and lipids, which must all stay intact in their composition and distribution. However, despite of this complexity, FS remain stable for three weeks which allows to perform several staining experiments from one preparation

3.3.2 Stability of fluorosomes upon freezing and re-thawing

In a next step we were interested to estimate the physical stability of fluorosomes (FS).

For that purpose five independent IL-2::GPI MA::GFP FS preparations were purified by ultracentrifugation and were resuspended in FACS buffer frozen at -80°C and re-thawed after 24 hours before their binding to HT-2 cells was determined and compared to freshly prepared FS. The FS showed remarkable stability upon freezing at – 80 °C and subsequent re-thawing since only a 8.8 ± 3.0 % loss of staining intensity with no loss in the number of positively identified cell numbers was apparent (Table 11).

In marked contrast, FS lost their ability to stain HT-2 cells within days when stored at room temperature or 37°C (not shown).

Sample	GeoMean (RT)	GeoMean (-80°C)	GeoMean (Δ in %)[a]	% positive (RT)	% positive (-80°C)	% positive (Δ in %)[b]
VLP #1	69	61	8	100	99,0	1,0
VLP #2	69	65	4	100	99,7	0,3
VLP #3	72	62	10	100	99,8	0,2
VLP #4	66	54	12	100	99,8	0,2
VLP #5	68	58	10	100	99,8	0,2
Mean	68,8	60	8,8	100	99,6	0,4
SD	± 2,2	±4,2	± 3,0	± 0	± 0,4	± 0,4

Table 11. Stability of IL-2 decorated fluorosomes (FS) upon freezing and re-thawing. [a] Reduction of geometric mean fluorescence intensities (geoMean) or [b] positively stained IL2 receptor expressing HT-2 cells upon freezing and re-thawing of fluorosomes. Data show mean values ± standard deviations from five independently performed experiments. GeoMeans of native HT-2 cells and HT-2 cells incubated with similar amounts of control FS were 2.6 ± 0.4 and 4.6 ± 0.5, respectively.

3.4 Determination of binding affinities of the fluorosomes

The IL-2 receptor is composed of three chains, the α-chain (CD25), β-chain (CD122), and γ-chain (CD132). (67) The IL-2 receptor changes the affinity depending on the receptor components that are expressed, the low-affinity receptor (10^{-8}M) is only composed of the α-chain, the intermediate-affinity receptor (10^{-9}M) is composed of β- and γ-chain and the high-affinity receptor is composed of all three chains. (67, 71, 77, 79, 129-131) While the intermediate-affinity receptor is constitutively expressed on resting T cells the high-affinity receptor expression is induced upon T cell activation. (67, 71, 132) Because of this affinity differences, we asked if it would be possible to detect this binding differences with the fluorosomes (FS) via flow cytometry. The read out cells for these experiments were HEK-293 cells. Therefore this cancer cell line was transiently transfected with the decoration constructs. The IL-2 receptor variants were tested by two different ways: (i) by the transfection of HEK-293 cells with receptor components followed by staining with IL-2::GPI MA::GFP FS and (ii) by the opposite situation: IL-2::GPI transfected HEK-293 cells stained with IL-2 receptor decorated FS.

3.4.1 Molecular details of the applied GPI-anchored Interleukin receptor-components

The GPI-anchor CD16b was fused to the extracellular (Tab.2) domains of IL-2 receptor chains.

Chains	construct length	molecular weight
α-chain (CD25)	858 bp	50-60 kDa
β-chain (CD122)	857 bp	70-80 kDa
γ-chain (CD132)	899 bp	60-70 kDa

Table 12. The IL-2 receptor chains fused to the GPI-anchor of CD16b with a length of 138bp. (The length and weight of the constructs include also the GPI-anchor).

3.4.2 Expression control of GPI-anchored α-chain (CD25)

In a next step we wanted to know if the GPI-anchored α-chain (CD25) of the IL-2 receptor is expressed on HEK-293 cells and their secreted VLP.

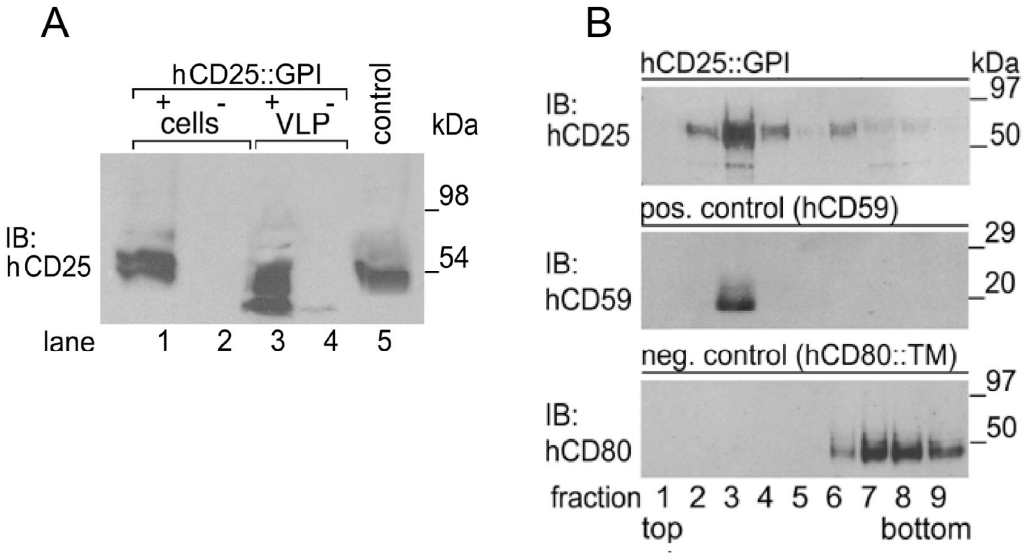

Figure 14. Immunoblot of the α-chain (CD25) on transfected HEK-293 cells and VLP. (A) are cell lysates and the corresponding VLP from CD25 transfected and control transfected HEK-293, the positive control are activated human PBMC. The isopycnic sucrose gradient (B) of CD25 transfected HEK-293, the positive control CD59 and the negative control CD80.

To investigate the expression of α-chain (CD25), HEK-293 cells were Ca_2PO_4-transfected with the construct and with gag/pol (OGP) for VLP budding. The cells were lysed and the corresponding VLP were purified, three days after transfection with α-chain (CD25). Furthermore, we looked due to isopycnic sucrose gradient centrifugation for lipid rafts targeting of the construct.

The results of the Western blot (Fig.14A) show the clear expression of the α-chain (CD25) on the transfected HEK-293 cells and also on their secreted VLP, on the other hand mock control-transfected cells and VLP don`t show any signal. The positive control are coated beads (anti CD3/CD28) activated human PBMC. The signal of the α-chain (CD25) in the immunoblot is strong and at the expected high of ~ 60 kDa. The VLP show also clear targeting of the construct. Moreover, the results (Fig. 14B) of the sucrose gradient centrifugation reveal a clear-cut lipid raft targeting of the α-chain (CD25), which is mainly contained in fraction two and three. The positive control is CD59, which is lipid raft targeted. The negative

control is the CD80 which is clearly not lipid raft targeted and contained in fraction 6-9. The Western blots of Figure 14 demonstrate the expression of the GPI-anchored α-chain (CD25). in transfected HEK-293, in the VLP and show also significant lipid raft targeting.

3.4.3 Phosphatidylinositol phospholipase C releases the GPI-anchor from Interleukin-2 receptor-components

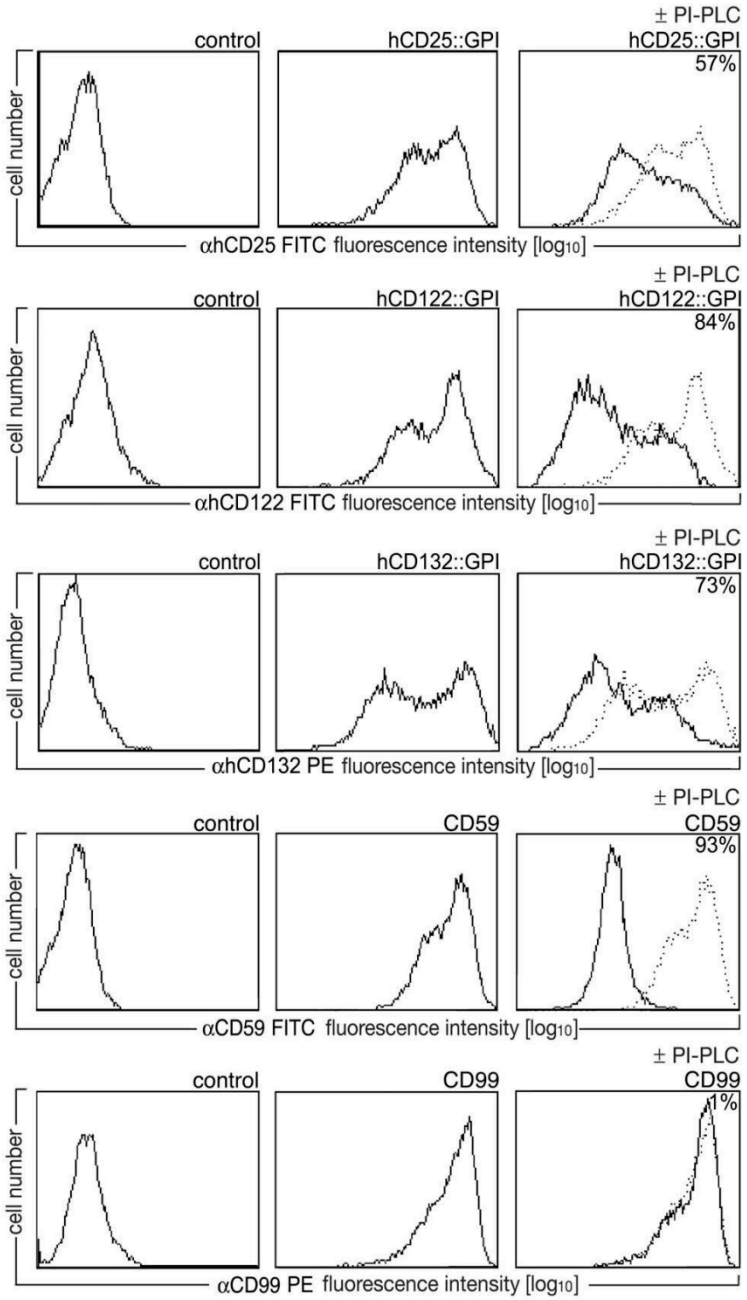

Figure 15. PI-PLC release of human IL-2 receptor GPI-anchored chains. The three upper histograms correspond to the human IL-2 receptor chains. CD59 is a GPI-anchored receptor, corresponds to the positive control, CD99 is a transmembrane receptor used as negative control. The percentage values correspond to the release of the receptors.

While GPI-anchoring of our constructs is essential for the targeting to the lipid rafts and such the budding into the VLP we investigated the anchoring by phosphatidylinositol phospholipase C (PI-PLC) release and analyses by flow cytometry. GPI-anchored constructs treated with PI-PLC are released and can as result no longer be detected by flow cytometry.

In order to check the constructs release after the PI-PLC treatment HEK-293 cells were Ca_2PO_4-transfected with the α-chain (CD25), the β-chain (CD122) and the γ-chain (CD132). Three days after the transfection HEK-293 cells were detached from the culture plate and afterwards separated in two groups. The first group was treated with PI-PLC the second group was left untreated and such used as positive control. The treatment with PI-PLC requires an incubation time of 2 hours at 37°C.

Figure 15 shows the flow cytometric analyses of the PI-PLC release of the three constructs (α-, β-, γ-chain), their untreated positive control, the CD59 positive control and the CD99 negative control. The α-chain (CD25) reveals the weakest release of 57 % compared to 84 % of β-chain (CD122) and 73 % of γ-chain (CD132). However, despite of the only weaker release of the α-chain (CD25) compared to the β-chain (CD122) and the γ-chain (CD132), this experiment shows a significant decreased signal which let us conclude that the modified receptors show a clear-cut GPI-anchoring. The CD59 is a naturally GPI-anchored molecule and is therefore used as positive control which reveals a release of 93 %. The CD99 is a naturally transmembrane receptor, and is therefore not released by the PI-PLC (release 1%). The controls CD59 and CD99 give a hint, concerning the specificity of the PI-PLC release.

The PI-PLC release experiments show that the developed constructs that we use in our experiments are to a significant amount GPI-anchored.

3.4.4 Fluorosomes decorated with Interleukin-2 stain human embryonic kidney-293 cells transfected with Interleukin-2 receptor-components

After having shown on HT-2 cells that it is in principle possible to visualize receptor-ligand interactions using fluorosomes (FS), we wanted further to assess, if we could also detect different binding affinities.

For that purpose, we have Ca_2PO_4-transefcted HEK-293 cells with different chain combinations, the intermediate-affinity receptor (βγ-chain) and the high affinity receptor (αβγ-chain), of the IL-2 receptor and stained them with IL-2::GPI MA::GFP FS (IL-2::GPI FS) to evaluate their binding capacity. The HEK-293 read out cells were prepared three day after transfection for the flow cytometry analyses by setting the cell number to 5 x 10^6 cells per ml. The MA::GFP stable producer cells were transfected with gag/pol (OGP) and IL-2::GPI. The secreted IL-2::GPI FS were purified from the supernatant, incubated for 30 minutes with the readout cells, washed once with FACS buffer and analyzed by flow cytometry.

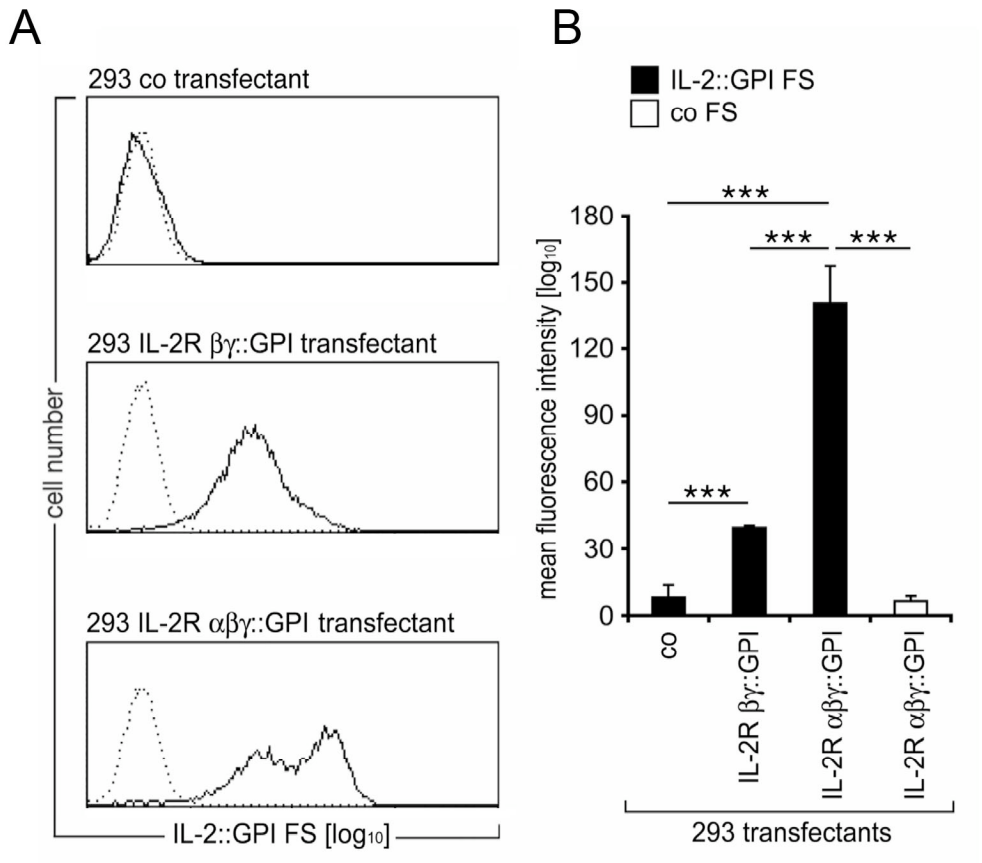

Figure 16. IL-2::GPI FS discriminate between target cells expressing low- or high-affinity IL-2 receptor. (A) Panel shows overlay histograms of HEK-293 cells transfected with control plasmid (upper panel), IL-2 receptor βγ-chain (middle panel) or IL-2 receptor αβγ-chain (lower panel) stained with either IL-2::GPI (solid line) or control (dotted line) FS. (B) Geometric MFI-values of indicated HEK-293 cell transfectants stained with IL-2::GPI (black bars) or control (white bar) FS from three independently performed experiments + SD are shown. Statistical significance was calculated by the paired, two-tailed Student's t-test; *** $p < 0.001$.

As stated above, the main question of the experiment is: Are we able to detect different binding affinities with the help of IL-2::GPI decorated fluorosomes? The

overlay histograms (Fig.16) document the binding difference of IL-2::GPI FS on HEK-293 cells transfected with intermediate- or the high-affinity receptor.

This experiment mirrors the natural affinities of the IL-2 receptor. While control-FS show no signal and βγ-transfected HEK-293 cells show an intermediate binding affinity the αβγ-transfected HEK-293 cells yield a high affinity signal (Fig. 16A). The results of three independent experiments are summed up in Figure 16B showing the differences in geo MFI of the used FS preparations.

In conclusion, the staining results validate the possibility to distinguish between cells expressing intermediate and high affinity receptors using FS. We can show very important characteristic of interleukin decorated FS: they cannot only detect single-chain receptors, they offer the possibility to detect cells expressing different states of multi-component receptors and distinguish between them.

3.4.5 Fluorosomes decorated with different Interleukin-2 receptor components stain Interleukin-2::GPI transfected human embryonic kidney-293 cells

The next question was, if it would be possible to perform the experiments described *vice versa*.

For that purpose we used fluorosomes (FS) decorated with IL-2 receptor components to stain HEK-293 expressing IL-2::GPI. We transfected HEK-293 with IL-2::GPI, and cultured them for three days, detached them and set them to a cell number of 5 x 10^6 cells per ml. For FS production stable HEK-293 MA::GFP cells were transfected with gag/pol (OGP) and different receptor combinations. Four different preparations were generated: control FS, FS decorated with the low affinity IL-2 receptor (β-chain::GPI), FS decorated with the intermediate (βγ-chain::GPI) and high-affinity IL-2 receptor (αβγ-chain::GPI).

Thus transfected MA::GFP cells were cultured for three days and FS, were purified and used for staining from the supernatant. The IL-2 decorated HEK-293 read out cells were incubated with the respective FS preparations for 30 minutes at RT, washed with FACS buffer and analyzed by flow cytometry.

As expected from the different published binding affinities, the results of Figure 17, show also variation in the binding of the respective FS preparations to IL-2::GPI transfected read-out cells. The staining intensities can be distinguished between low signal only from the γ-chain::GPI FS, intermediate signal from βγ-chain::GPI

FS and high signal from the complete receptor (αβγ-chain::GPI FS) (Fig. 17 A). The Figure 17B shows the statistical analyses of three independently performed staining experiments. This abstract model system confirms that we are able to use FS as platform for multi-protein complexes and receptors, because interleukin are not physiologically cell membrane associated.

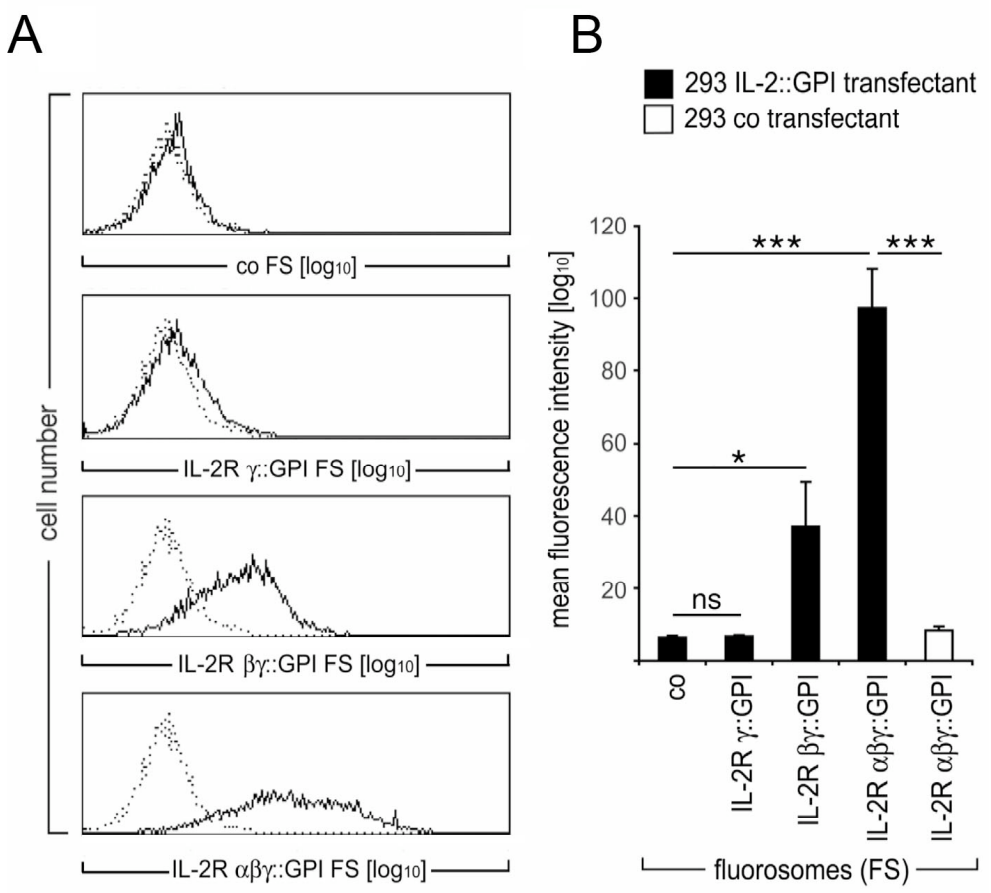

Figure 17. FS decorated with complex combinations of the IL-2 receptor bind to target cells expressing membrane-bound IL-2. (A) Panel shows overlay histograms of HEK-293 cells expressing membrane-bound IL-2::GPI, which were incubated with control FS (upper panel), IL-2 receptor γ-chain::GPI FS (upper-middle panel), IL-2 receptor βγ-chain::GPI FS (lower-middle panel), or IL-2 receptor αβγ-chain::GPI FS (lower panel), respectively (bold lines). Dotted lines represent fluorescence of control transfected HEK-293 cells incubated with the respective FS. (B) Geometric mean fluorescence values of IL-2::GPI (black bars) or control (white bar) HEK-293 transfectants stained with the indicated FS from three independently performed experiments + SD are shown. Statistical significance was calculated by the paired, two-tailed Student's t-test; ns $p > 0.05$; * $p < 0.05$; *** $p < 0.001$.

3.5 Identification of human peripheral blood cells with fluorosomes

3.5.1 Interleukin-2::GPI fluorosomes identify activated human peripheral blood cells expressing Interleukin-2 receptor α-chain (CD25)

In this part of our work we wanted to know, if it is possible to identify receptor expression on peripheral blood cells of healthy donor which were activated with anti-CD3/CD28 coated beads.

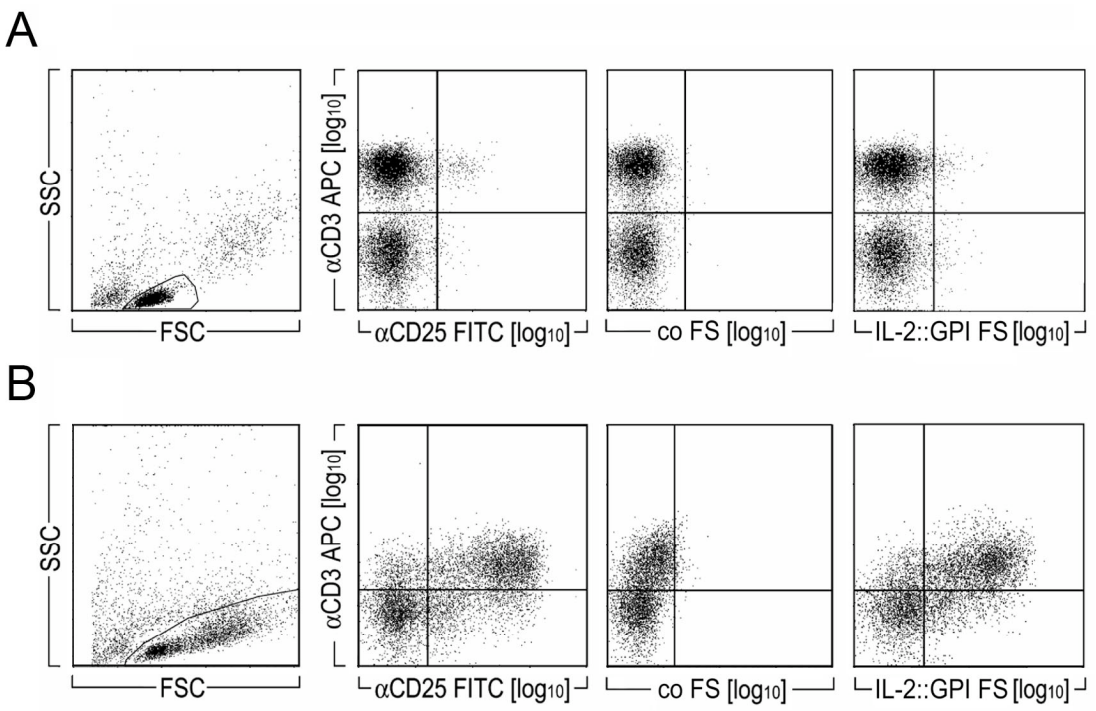

Figure 18. IL-2::GPI FS identify activated T lymphocytes. Two-parameter dot plot analyses of freshly isolated (A) or activated (CD3/CD28 coated beads, 48 hours) (B) PBMC upon incubation with IL-2::GPI FS, control FS, or CD25 FITC-conjugated mAb and counterstained with a CD3 APC-conjugated mAb are shown. Gating for lymphocytes was performed according to typical FSC/SSC-characteristics. Markers were set according to non binding control mAb or control FS. Data are representative of three experiments.

For that purpose, we first tried to verify if is it, possible to stain directly isolated human blood cells. The cells used for the experiment are peripheral blood mononuclear cells (PBMC). The PBMC fraction contains lymphatic cells like T and B cells and monocytes and are directly isolated from human blood. In primary experiments resting and activated PBMC were used. In order to stimulate up

regulation of CD25 and thus gain a better read-out for staining with IL-2::GPI MA::GFP FS (IL-2::GPI FS). The resting PBMC were used as negative control. PBMC were activated with anti_ CD3/ CD28 coated beads and cultured 48 hours before the experiment. The beads (3 beads/cell) lead to activation of the T cell by inducing the first signal with anti_CD3 and the second signal with anti_CD28. The activation time of 48 hours is important for the PBMC as this is the optimal time-point for the up-regulation of the IL-2 receptor α-chain.

Proper activation was checked by microscopy of resting PBMC compared to activated PBMC and revealed for activated cells clustering and high cell number. Staining of the IL-2::GPI FS on resting and activated PBMC was compared to α-chain (CD25) stained resting and activated PBMC.

In order to add a better resolution to detection, we used an anti_CD3 antibody to specifically stain T cells. In a double staining of resting PBMC we can thus detect an upper T cell population that is positive for CD3 and negative for the IL-2 receptor. In contrast, activated T cells should be double positive in a dot plot, for CD3 and the IL-2 receptor.

Figure 18A shows that resting $CD3^+$ T cells are negative for control FS and anti_CD25 and IL-2::GPI FS. The anti_CD25 control antibody, but also the IL-2::GPI FS reveal a small T cell population of CD25 receptor positive cells, which are presumably regulatory T cells (T_{reg}). T cells always contain small amounts of T_{reg}. The important feature of these cells is their constitutive IL-2 receptor expression, which allows them to become potent consumers of IL-2. (121)

Figure 11B shows that activated $CD3^+$ T cells shift in the dot plot when using either the anti_CD25 antibody or IL-2::GPI FS. The side scatter (SSC) and the forwards scatter (FSC) gate for the proliferating T cells was changed because of the new cell morphology induced by activation which leads to a different cellular autofluorescence.

These experimental results of the PBMC staining reveal clear-cut staining by FS, comparable to staining with antibodies. Moreover, the decoration with IL-2 offers the possibility for detection of other cell populations that are not detectable by staining for one chain of the IL-2 receptor like the anti_CD25 antibody. This let us to the conclusion that the FS staining method will offer new detection and interpretation levels.

3.5.2 Interleukin-7::GPI fluorosomes identify resting human peripheral blood cells expressing Interleukin-7 receptors

In a new step we wanted to know if it is possible to use other Interleukins. Different Interleukins will give the opportunity to stain cells that have other receptors as marker. Interleukin-7 was chosen for the decoration of the FS. The IL-7 molecule has all suitable criteria for the decoration of FS, it has a high affinity to it`s receptor and is an interleukin with well-described role, for example in T and B cell development and homeostasis. (99, 112-114)

For these purpose we assessed IL-7 decorated FS using resting PBMC as read-out cell. The isolation of PBMC from whole blood from healthy donors was performed as usual, but PBMC were not activated with beads. The IL-7::GPI MA::GFP FS (IL-7::GPI FS) were produced similar to IL-2::GPI MA::GFP FS (IL-2::GPI FS), by the transiently transfection of stable HEK-293 MA::GFP cells with gag/pol (OGP) and IL-7::GPI followed by purification three days after transfection. Staining and analyses were performed as described in Material and Methods.

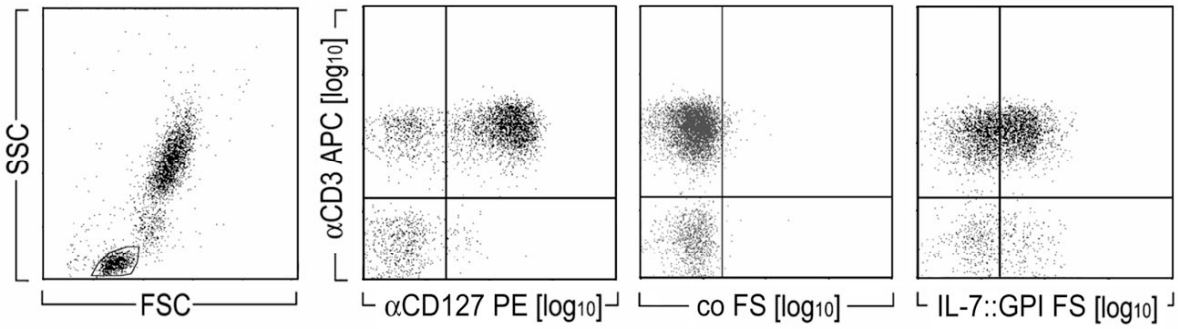

Figure 19. IL-7::GPI FS identify activated T lymphocytes. Two-parameter dot-plot analyses of whole blood cells gated on lymphocytes of a representative healthy donor incubated with IL-7::GPI FS, control FS or CD127 PE conjugated mAb and counterstained with CD3 APC-conjugated mAb are shown.Lymphocytes were gated according to typical FSC/SSC characteristics. Data are representative of four experiments.

The IL-7 receptor is composed of two chains, the CD127 and the common γ-chain (CD132). Thus we used an anti_CD127 antibody as positive control.

Both cells the positive control and IL-7::GPI FS show a clear-cut staining of the IL-7 receptor compared to the negative control FS (Fig. 19). The direct comparison between the IL-7::GPI FS and the anti_CD127 shows a stronger staining of the antibody. However, the detection of the IL-7 receptor with the IL-7::GPI FS is possible and clearly distinguishable from negative control FS. Moreover, the IL-

7::GPI FS also seem to detect another cell population that are CD3/CD127 negative but express an IL-7 receptor. The specific binding of the IL-7 decorated FS could be shown by experiments using soluble IL-7 as competitive inhibitor for FS binding (data not show).

3.5.3 Interleukin-2::GPI fluorosomes identify malignant B cells in human peripheral blood cells of chronic lymphocytic leukemia-patients

The last part included experiments which show FS used in a diagnostic context. Therefore we decided to stain chronic lymphocytic leukemia (CLL) B cells with IL-2::GPI FS. B cells from many CLL patients express the IL-2 receptor on the cell surface. One of the characteristic markers for the routine detection of CLL, therefore is CD25.

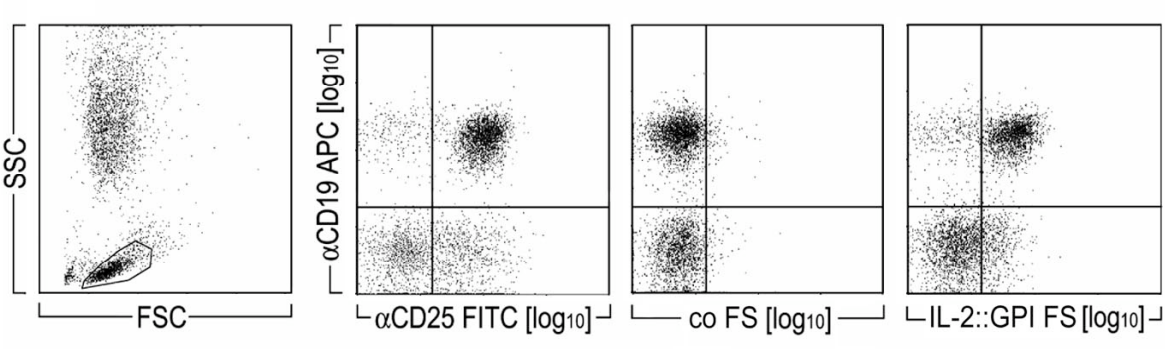

Figure 20. IL-2::GPI FS identify CLL B cells. Whole blood of a CLL-patient was stained with IL-2::GPI FS, control FS or CD25 FITC-conjugated mAb and counterstained with a CD19 APC-conjugated mAb. Lymphocytes were gated according to typical FSC/SSC characteristics. Markers were set according to staining of non binding control mAb or control FS. Data are representative of multiple individuals (n=11).

Detection of CLL B cells was done directly in whole blood with IL-2::GPI FS which means that the PBMC were not isolated compared to the other experiments described above. We did not know, if our FS system would work in this case. However whole blood staining protocols with antibodies are used routinely in diagnostic laboratories. Staining of whole blood samples contains some critical steps for FS, for example the lysis of the erythrocytes. This lysis step, using LYSE-solution which leads to the remove of erythrocytes, in whole blood staining procedure, could be problematic for the FS. The LYSE-solution could probably degrade the FS. Another problem could be reactivity of some blood components with the FS which could have a negative influence on the staining result.

However, the procedure for the whole blood staining is less complex compared to the staining of isolated PMBC.

For this purpose blood samples were incubated for 30 minutes at RT with the anti_CD25 antibody and IL-2::GPI FS. Afterwards the lysis step with LYSE-solution was performed followed by wash step with bi-distillated water (ddH_20) and was analyzed by flow cytometry. For the specific detection of the B cells in the whole blood staining an anti_CD19 antibody was used. CD 19 is a component of the complement receptor and specific marker for B cells. (69,70)

Figure 20 shows one staining of a representative CLL-patient. The positive control antibody and the IL-2::GPI FS shows a clear-cut binding to $CD19^+$ cells in the dot plot compared to control-transfected FS. This experiment proves that B cell blasts from CLL-patients can be clearly detected with IL-2::GPI FS. The staining of the patients was done by routine protocols, which demonstrates the simple handling of our staining tool. In general it does not seem as if there are unexpected interference with whole blood components or staining reagents components.

4 Discussion

The most important coordinated response against infectious microbes is provided by the immune-system (70). Moreover, it represents one of the best organized systems developed during evolution. The complexity of the system is not only marked by its memory capacity but also by its adaptivity, which leads to the production of antigen-specific antibodies. (69, 70) Antibodies are remarkable molecules concerning their diversity and their specificity, which allows the recognition and the binding of an enormous range of antigen. (70) These properties of antibodies are the reason for their broad diagnostic application, which allows to detect specific epitopes on cells or tissues. The disadvantages of antibodies as staining tools are their production which is connected with some difficulties. One problem is the usage of animals as producer organism, which is time-consuming and ethically problematic. Typical producer animals are rabbits, mice or rats. The production method of monoclonal antibodies with known specificity in animals was first described by George Köhler and Cesar Milstein 1975. (70) This technique of antibody production requires purified antigens, which is injected into the producer organism. (70) Polyclonal B cells are first isolated from the spleen of the producer organism and afterwards immortalized by fusion with a mutant myeloma line, which leads to an immortalized hybridoma cell line. (70) These hybridoma cells are screened for the production of monoclonal antibodies. (70) The input of work required for the production of fluorosomes (FS) and antibodies is not comparable. Our complete production is based on *in-vitro* cell culture and does not require stock breeding with animals. The production of FS requires only the stable HEK-293 MA::GFP cell line, the retroviral core proteins (e.g. MoMLV gag/pol) and the respective immune-receptors. The purified FS can be used like antibodies and they also have a high degree of stability.

There also exist other staining tools basing on the same principle that were presented in the past. One of these are Moloney murine leukemia viruses with SU protein which is fused the GFP (SU-GFP). (134) The fluorescent dye is targeted into the lipid raft and incorporated into the infectious virus. This staining tool was used to show virus infection of target cells. The fluorescent VLP developed in our laboratory are used in another context: we want to show specific binding of the FS to the target cells. But we can say that our tool is an improved version compared to above described infectious SU-GFP MoMLV. The FS developed in our

laboratory contain an anchor for the fluorescent dye in the inner leaflet of the VLP and is not exposed on the outer leaflet like the SU-GFP. (134) The exposed SU-GFP could be problematic in our system as it would interfere or even inhibit receptor/ligand interactions.

Another derivate of our system are decorated VLP from MoMLV with GFP fused to a GPI-anchor. (136) In contrast to SU-GFP MoMLV the second possibility of targeting GFP has the advantage that the produced particles are non-infectious. The disadvantage of GFP::GPI is the exposition in the outer leaflet of the VLP, which is problematic.

Another staining tool that was shown in past were GFP conjugated interleukins or interleukins that were directly labeled with fluorescent dyes. (135) These interleukins give also the possibility to show interactions between receptor and corresponding ligand. The main disadvantage of conjugated interleukins is the low signal intensity. The signal intensity which is emitted by the FS is relatively high because of the big VLP platform which contains a large amount of fluorescent dye. Moreover, this platform allows us not only to enhance the signal, but also to target multi complex molecules.

Our experiments demonstrate that our newly developed, FS - based system allows the staining of different cells, which express the specific ligand on the cell surface.

In a first step we showed the preferential targeting of MA::GFP to the cell membrane of transfected HEK-293 cells, while GFP was mostly equally distributed in the cytosol of the cell. For that purpose we used microscopy analyses (Fig.8) and biochemical analyses (Fig.9). The microscopy results show a localization of GFP to the membrane in the case of the MA::GFP stable producer cells. The biochemical analyses using isopycnic sucrose gradients, which separates the cell components due to their density gives us the evidence for the targeting of the MA::GFP to the lipid raft fractions. Furthermore, the other components like IL-2::GPI and gag/pol (OGP) were also successfully shown to be targeted to lipid rafts due to isopycnic sucrose gradient analyses (Fig.9). Thus, we have clearly demonstrated the lipid raft targeting of our components, which is the main condition for budding into the FS.

The next step was to test the staining efficiency and the specificity of the IL-2::GPI decorated MA::GFP FS also compared to IL-2::GPI decorated GFP FS. These experiments confirmed the high staining efficiency and also the specificity of IL-

2::GPI decorated FS, which was demonstrated in inhibition experiments using soluble IL-2 (Fig.10). We decided to perform these experiments using HT-2 cells expressing constitutively the mIL-2 receptor on the cell surface which give us a stable read-out and make us independent of transfection efficiency. Therefore, this cell line was important to develop the system and perform primary experiments.

The next interesting point for us was the evaluation of particle stability. We tested two major parameters, time and temperature stability. Evaluation of these parameters is the prerequisites and at the same time possible barriers for further experiments with the FS. The reason why we gave the stability experiments such an important role is the application in routine diagnostics, which requires high fidelity of the staining tool. Our stability experiments (Tab. 11 and 12) reveal that fluorescence activity and staining intensity remain virtually the same when FS are stored at 4 °C. Moreover particles seem not to lose activity after freezing at – 80 °C.

A further idea was to test differences in binding affinity. For that purpose we set up a model system either by the decoration of FS with IL-2::GPI on HEK-293 with receptor-components (Fig.16) or FS decorated with receptor-components on IL-2::GPI transfected HEK-293 (Fig.17). Both experiments revealed differences in FS binding, which give a hint about the binding specificity and affinity. However, we showed the difference of the binding affinities between the intermediate- and the high- binding affinity IL-2 receptor. We discovered that IL-2 receptor-components transfected HEK-293, with the intermediate (βγ-chain) and the high affinity receptor (αβγ-chain) can be distinguished with the help of IL-2 decorated FS. The reached geo MFI of 50 for the intermediate affinity IL-2 receptor and a geo MFI of 150 for the high affinity IL-2 receptor revealed this clear-cut difference in the binding affinities. Moreover, we were able to see this difference, the other way round. Interleukin-2::GPI transfected HEK-293 were stained with decorated FS with the low affinity (γ-chain::GPI), the intermediate (βγ-chain::GPI) and the high affinity (αβγ-chain::GPI) receptor. The result of the stainings were comparable to the experiment shown in Figure 16. The low affinity receptor reveals almost no significant signal. The intermediate chain leads to a geo MFI of 50 and the high affinity receptor to a geo MFI of 100. The last but most relevant experiment is the staining of PBMC from healthy and CLL patients with IL-2 and IL-7 decorated FS.

The staining of human blood cells is one of our main aims, because this may lead to diagnostic application of FS.

At first we analyzed if it is possible to detect the expression of the high affinity IL-2 receptor on activated and non-activated PBMC isolated from healthy donors with IL-2::GPI decorated FS (Fig.18). Activation of T cells using CD3/CD28 coated beads, leads to an up-regulation of the IL-2 receptor α-chain (CD25) which can be visualized with IL-2::GPI FS. This leads to a shift of $CD3^+$ T cells in the dot plot (Fig.18). Isolated PBMC used in this experiment do not contain other blood components like erythrocytes or serum proteins, which could have negative effects on the staining results. The next step was to stain PBMC from whole blood samples from CLL patients. The CLL patients´ malignant B cells are often IL-2 receptor positive. One characteristic marker used in diagnostic laboratories for the detection of CLL is CD25. Our routine laboratory has a long standing experience in the diagnosis of CLL patients, which gave us the opportunity to test different CLL patients blood stained with IL-2::GPI FS and standard reagents. The staining of the CLL B cell (Fig. 20) of one representative individual is shown, and indicates a clear position for both, the anti_CD25 antibody and IL-2::GPI FS. The detection of CLL B cells could be a first step to a diagnostic application of FS.

We showed also the detection of target cells with a second cytokine on FS. Staining of isolated resting PBMC was performed using IL-7::GPI decorated FS. (Fig. 19) These staining result showed strong binding of IL-7::GPI FS to $CD3^+$ T cells and demonstrates that FS can be decorated with a range of molecules. We also performed inhibition experiments with soluble IL-7 which leads to an inhibition of IL-7::GPI FS binding (data not shown). The inhibition indicates that the binding of IL-7::GPI FS is specific.

In summary, our experiments demonstrate the efficient lipid raft targeting of our constructs and the specific binding and high staining intensity of FS. Furthermore, we showed that FS are stable over time and at various storage temperatures and that it is possible to decorate FS with multi-subunit receptors and to stain different target cells.

Further potential applications of our particles could be the characterization of so far unknown receptor ligand interactions. Furthermore, the VLP platform can accommodate multi-subunit ligands or receptors, which are otherwise not easy to

express in the appropriate configuration and thus offers new perspectives for detection.

Disadvantages of our system are at the moment the transmembrane protein classes, while we are obligated to use derivates of type I transmembrane because of their orientation in the cell membrane. These proteins have to be liked to GPI-anchor to make sure that the transmembrane proteins are targeted into the lipid rafts. Another problem is the complexity of the FS, which is composed of different molecules and which might be problematic for the particle stability. Stability problems were, however, ruled out by the evaluation of the FS stability over the time which reveals that staining activity is assured for three weeks. Also the virus particle could be problematic because the virus envelope could probably interact with cell components and lead thereby to incorrect results.

In the future, we also hope to develop convenient expression strategies for type II, III and IV transmembrane proteins suitable for the membrane environment of FS.

Moreover, it will be interesting to explore the possibility to establish multicolor FS for double or triple staining purposes. The recently described ‘fruit’-colors developed by Roger Tsien and co-workers appear to be interesting candidates in that respect. (5) Another interesting point will be the direct staining of tissues with the FS that could be detected in microscopy.

Antibodies are very common and well established staining tools. However, we hope to supplement these detection systems with our FS. The FS possess all properties for a valuable staining tool, that can be easily meet the requirements to modified detected target cells of choice.

5 References

1. Derdak, S. V., H. J. Kueng, V. M. Leb, A. Neunkirchner, K. G. Schmetterer, E. Bielek, O. Majdic, W. Knapp, B. Seed, and W. F. Pickl. 2006. Direct stimulation of T lymphocytes by immunosomes: virus-like particles decorated with T cell receptor/CD3 ligands plus costimulatory molecules. *Proc Natl Acad Sci U S A 103:13144*.
2. Kueng, H. J., V. M. Leb, D. Haiderer, G. Raposo, C. Thery, S. V. Derdak, K. G. Schmetterer, A. Neunkirchner, C. Sillaber, B. Seed, and W. F. Pickl. 2007. General strategy for decoration of enveloped viruses with functionally active lipid-modified cytokines. *J Virol 81:8666*.
3. Leb, V. M., B. Jahn-Schmid, K. G. Schmetterer, H. J. Kueng, D. Haiderer, A. Neunkirchner, G. F. Fischer, K. Nissler, A. Hartl, J. Thalhamer, B. Bohle, B. Seed, and W. F. Pickl. 2008. Molecular and functional analysis of the antigen receptor of Art v 1-specific helper T lymphocytes. *J Allergy Clin Immunol 121:64*.
4. Heim, R., and R. Y. Tsien. 1996. Engineering green fluorescent protein for improved brightness, longer wavelengths and fluorescence resonance energy transfer. *Curr Biol 6:178*.
5. Shaner, N. C., R. E. Campbell, P. A. Steinbach, B. N. Giepmans, A. E. Palmer, and R. Y. Tsien. 2004. Improved monomeric red, orange and yellow fluorescent proteins derived from Discosoma sp. red fluorescent protein. *Nat Biotechnol 22:1567*.
6. Shimomura, O., F. H. Johnson, and Y. Saiga. 1962. Extraction, purification and properties of aequorin, a bioluminescent protein from the luminous hydromedusan, Aequorea. *J Cell Comp Physiol 59:223*.
7. Coffin, J., A. Haase, J. A. Levy, L. Montagnier, S. Oroszlan, N. Teich, H. Temin, K. Toyoshima, H. Varmus, P. Vogt, and et al. 1986. What to call the AIDS virus? *Nature 321:10*.
8. Coffin, J. W., R. Dhillon, R. G. Ritzel, and F. E. Nargang. 1997. The Neurospora crassa cya-5 nuclear gene encodes a protein with a region of homology to the Saccharomyces cerevisiae PET309 protein and is required in a post-transcriptional step for the expression of the mitochondrially encoded COXI protein. *Curr Genet 32:273*.
9. Lee, P. P., and M. L. Linial. 1994. Efficient particle formation can occur if the matrix domain of human immunodeficiency virus type 1 Gag is substituted by a myristylation signal. *J Virol 68:6644*.
10. Wills, J. W., R. C. Craven, R. A. Weldon, Jr., T. D. Nelle, and C. R. Erdie. 1991. Suppression of retroviral MA deletions by the amino-terminal membrane-binding domain of p60src. *J Virol 65:3804*.
11. Lodish, H., A. Berk, S. L. Zipursky, and J. Darnell. 2001. *Molekulare Zellbiologie*. Spektrum.
12. Plattner, H., and J. Hentschel. 2002. *Zellbiologie*. Thieme.
13. Murakami, T., R. Yumoto, J. Nagai, and M. Takano. 2002. Factors affecting the expression and function of P-glycoprotein in rats: drug treatments and diseased states. *Pharmazie 57:102*.
14. Devasahayam, M. 2007. Factors affecting the expression of recombinant glycoproteins. *Indian J Med Res 126:22*.
15. Lewin, B. 2000. *Genes*. Oxford University Press.
16. Appenzeller-Herzog, C., and H. P. Hauri. 2006. The ER-Golgi intermediate compartment (ERGIC): in search of its identity and function. *J Cell Sci 119:2173*.
17. Yewdell, J. W., U. Schubert, and J. R. Bennink. 2001. At the crossroads of cell biology and immunology: DRiPs and other sources of peptide ligands for MHC class I molecules. *J Cell Sci 114:845*.
18. Higy, M., T. Junne, and M. Spiess. 2004. Topogenesis of membrane proteins at the endoplasmic reticulum. *Biochemistry 43:12716*.
19. Spiess, M. 1995. Heads or tails--what determines the orientation of proteins in the membrane. *FEBS Lett 369:76*.
20. von Heijne, G., and Y. Gavel. 1988. Topogenic signals in integral membrane proteins. *Eur J Biochem 174:671*.
21. Berg, J. M., J. L. Tymoczko, and L. Stryer. 2003. *Biochemie*. Spektrum.
22. Paulick, M. G., and C. R. Bertozzi. 2008. The glycosylphosphatidylinositol anchor: a complex membrane-anchoring structure for proteins. *Biochemistry 47:6991*.
23. Maeda, Y., H. Ashida, and T. Kinoshita. 2006. CHO glycosylation mutants: GPI anchor. *Methods Enzymol 416:182*.

24. Ferguson, M. A., S. W. Homans, R. A. Dwek, and T. W. Rademacher. 1988. Glycosyl-phosphatidylinositol moiety that anchors Trypanosoma brucei variant surface glycoprotein to the membrane. *Science 239:753*.
25. Homans, S. W., M. A. Ferguson, R. A. Dwek, T. W. Rademacher, R. Anand, and A. F. Williams. 1988. Complete structure of the glycosyl phosphatidylinositol membrane anchor of rat brain Thy-1 glycoprotein. *Nature 333:269*.
26. Ikezawa, H. 2002. Glycosylphosphatidylinositol (GPI)-anchored proteins. *Biol Pharm Bull 25:409*.
27. Low, M. G. 1989. The glycosyl-phosphatidylinositol anchor of membrane proteins. *Biochim Biophys Acta 988:427*.
28. Hebert, D. N., S. C. Garman, and M. Molinari. 2005. The glycan code of the endoplasmic reticulum: asparagine-linked carbohydrates as protein maturation and quality-control tags. *Trends Cell Biol 15:364*.
29. Shakin-Eshleman, S. H., S. L. Spitalnik, and L. Kasturi. 1996. The amino acid at the X position of an Asn-X-Ser sequon is an important determinant of N-linked core-glycosylation efficiency. *J Biol Chem 271:6363*.
30. Viejo-Borbolla, A., M. Pizzato, E. D. Blair, and T. F. Schulz. 2005. Insertion of targeting domains into the envelope glycoprotein of Moloney murine leukemia virus (MoMLV)-based vectors modulates the route of mCAT-1-mediated viral entry. *Virus Res 108:45*.
31. Rajendran, L., and K. Simons. 2005. Lipid rafts and membrane dynamics. *J Cell Sci 118:1099*.
32. Munro, S. 2003. Lipid rafts: elusive or illusive? *Cell 115:377*.
33. Sengupta, P., B. Baird, and D. Holowka. 2007. Lipid rafts, fluid/fluid phase separation, and their relevance to plasma membrane structure and function. *Semin Cell Dev Biol 18:583*.
34. Patra, S. K., and S. Bettuzzi. 2007. Epigenetic DNA-methylation regulation of genes coding for lipid raft-associated components: a role for raft proteins in cell transformation and cancer progression (review). *Oncol Rep 17:1279*.
35. Barquinero, J., H. Eixarch, and M. Perez-Melgosa. 2004. Retroviral vectors: new applications for an old tool. *Gene Ther 11 Suppl 1:S3*.
36. Schlegel, H. G. *Allgemeine Mikrobiologie*. Thieme.
37. Madigan, M. T., J. M. Martinko, J. Parker, and T. D. Brock. 2002. *Brock Mikrobiologie*. Spektrum.
38. Olsen, K. E., and K. B. Andersen. 1999. Palmitoylation of the intracytoplasmic R peptide of the transmembrane envelope protein in Moloney murine leukemia virus. *J Virol 73:8975*.
39. Battini, J. L., J. M. Heard, and O. Danos. 1992. Receptor choice determinants in the envelope glycoproteins of amphotropic, xenotropic, and polytropic murine leukemia viruses. *J Virol 66:1468*.
40. Einfeld, D., and E. Hunter. 1988. Oligomeric structure of a prototype retrovirus glycoprotein. *Proc Natl Acad Sci U S A 85:8688*.
41. Pinter, A., and E. Fleissner. 1979. Structural studies of retroviruses: characterization of oligomeric complexes of murine and feline leukemia virus envelope and core components formed upon cross-linking. *J Virol 30:157*.
42. Thomas, D. J., J. S. Wall, J. F. Hainfeld, M. Kaczorek, F. P. Booy, B. L. Trus, F. A. Eiserling, and A. C. Steven. 1991. gp160, the envelope glycoprotein of human immunodeficiency virus type 1, is a dimer of 125-kilodalton subunits stabilized through interactions between their gp41 domains. *J Virol 65:3797*.
43. Witte, O. N., and D. F. Wirth. 1979. Structure of the murine leukemia virus envelope glycoprotein precursor. *J Virol 29:735*.
44. Hausmann, J., D. Ortmann, E. Witt, M. Veit, and W. Seidel. 1998. Adenovirus death protein, a transmembrane protein encoded in the E3 region, is palmitoylated at the cytoplasmic tail. *Virology 244:343*.
45. Hensel, J., M. Hintz, M. Karas, D. Linder, B. Stahl, and R. Geyer. 1995. Localization of the palmitoylation site in the transmembrane protein p12E of Friend murine leukaemia virus. *Eur J Biochem 232:373*.
46. Schmidt, M., M. F. Schmidt, and R. Rott. 1988. Chemical identification of cysteine as palmitoylation site in a transmembrane protein (Semliki Forest virus E1). *J Biol Chem 263:18635*.
47. Veit, M., M. F. Schmidt, and R. Rott. 1989. Different palmitoylation of paramyxovirus glycoproteins. *Virology 168:173*.
48. Yang, C., and R. W. Compans. 1996. Palmitoylation of the murine leukemia virus envelope glycoprotein transmembrane subunits. *Virology 221:87*.

49. Valsesia-Wittmann, S., F. J. Morling, T. Hatziioannou, S. J. Russell, and F. L. Cosset. 1997. Receptor co-operation in retrovirus entry: recruitment of an auxiliary entry mechanism after retargeted binding. *Embo J 16:1214*.
50. Valsesia-Wittmann, S., F. J. Morling, B. H. Nilson, Y. Takeuchi, S. J. Russell, and F. L. Cosset. 1996. Improvement of retroviral retargeting by using amino acid spacers between an additional binding domain and the N terminus of Moloney murine leukemia virus SU. *J Virol 70:2059*.
51. DeLarco, J., and G. J. Todaro. 1976. Membrane receptors for murine leukemia viruses: characterization using the purified viral envelope glycoprotein, gp71. *Cell 8:365*.
52. Kabat, D. 1989. Cell surface receptors for ecotropic murine retroviruses: mobile membrane proteins that mediate binding and slow endocytosis of the viral envelope glycoprotein. *Virology 171:467*.
53. Kielian, M., and S. Jungerwirth. 1990. Mechanisms of enveloped virus entry into cells. *Mol Biol Med 7:17*.
54. Baxter, E. W., K. Blyth, L. A. Donehower, E. R. Cameron, D. E. Onions, and J. C. Neil. 1996. Moloney murine leukemia virus-induced lymphomas in p53-deficient mice: overlapping pathways in tumor development? *J Virol 70:2095*.
55. Housset, V., and J. L. Darlix. 1996. Mutations at the capsid-nucleocapsid cleavage site of gag polyprotein of Moloney murine leukemia virus abolish virus infectivity. *C R Acad Sci III 319:81*.
56. Meyer, M. K., M. A. Nash, and R. B. Arlinghaus. 1995. Identification of a new viral protein containing CAp30 and NCp10 sequences in murine and feline leukemia retroviruses. *J Virol 69:1353*.
57. Arcement, L. J., W. L. Karshin, R. B. Naso, and R. B. Arlinghaus. 1977. "gag" polyprotein precursors of Rauscher murine leukemia virus. *Virology 81:284*.
58. Ledbetter, J. A., R. C. Nowinski, and R. N. Eisenman. 1978. Biosynthesis and metabolism of viral proteins expressed on the surface of murine leukemia virus-infected cells. *Virology 91:116*.
59. Ledbetter, J. A. 1979. Two-dimensional analysis of murine leukemia virus gag-gene polyproteins. *Virology 95:85*.
60. Auerbach, M. R., K. R. Brown, and I. R. Singh. 2007. Mutational analysis of the N-terminal domain of Moloney murine leukemia virus capsid protein. *J Virol 81:12337*.
61. Viejo-Borbolla, A., P. Thomas, E. D. Blair, and T. F. Schulz. 2005. Increase in infectivity of targeted Moloney murine leukemia virus-based gene-delivery vectors through lowering the threshold for fusion. *J Gen Virol 86:2469*.
62. Rein, A., M. R. McClure, N. R. Rice, R. B. Luftig, and A. M. Schultz. 1986. Myristylation site in Pr65gag is essential for virus particle formation by Moloney murine leukemia virus. *Proc Natl Acad Sci U S A 83:7246*.
63. Henderson, L. E., H. C. Krutzsch, and S. Oroszlan. 1983. Myristyl amino-terminal acylation of murine retrovirus proteins: an unusual post-translational proteins modification. *Proc Natl Acad Sci U S A 80:339*.
64. Schultz, A. M., and S. Oroszlan. 1983. In vivo modification of retroviral gag gene-encoded polyproteins by myristic acid. *J Virol 46:355*.
65. Bryant, M. L., R. O. Heuckeroth, J. T. Kimata, L. Ratner, and J. I. Gordon. 1989. Replication of human immunodeficiency virus 1 and Moloney murine leukemia virus is inhibited by different heteroatom-containing analogs of myristic acid. *Proc Natl Acad Sci U S A 86:8655*.
66. Graham, F. L., J. Smiley, W. C. Russell, and R. Nairn. 1977. Characteristics of a human cell line transformed by DNA from human adenovirus type 5. *J Gen Virol 36:59*.
67. Lin, J. X., and W. J. Leonard. 1997. Signaling from the IL-2 receptor to the nucleus. *Cytokine Growth Factor Rev 8:313*.
68. Morgan, D. A., F. W. Ruscetti, and R. Gallo. 1976. Selective in vitro growth of T lymphocytes from normal human bone marrows. *Science 193:1007*.
69. Janeway, C. A., P. Travers, and M. W. von Churchill Livingstone. 2002. *Immunobioloy*. Spektrum.
70. Abbas, A. B., A. H. Lichtman, and v. S. S.P. 2007. *Cellular and Molecular Immunology*.
71. Robb, R. J., A. Munck, and K. A. Smith. 1981. T cell growth factor receptors. Quantitation, specificity, and biological relevance. *J Exp Med 154:1455*.
72. Leonard, W. J., J. M. Depper, G. R. Crabtree, S. Rudikoff, J. Pumphrey, R. J. Robb, M. Kronke, P. B. Svetlik, N. J. Peffer, T. A. Waldmann, and et al. 1984. Molecular cloning and expression of cDNAs for the human interleukin-2 receptor. *Nature 311:626*.

73. Leonard, W. J., M. Kronke, N. J. Peffer, J. M. Depper, and W. C. Greene. 1985. Interleukin 2 receptor gene expression in normal human T lymphocytes. *Proc Natl Acad Sci U S A 82:6281*.
74. Ilangumaran, S., D. Finan, and R. Rottapel. 2003. Flow cytometric analysis of cytokine receptor signal transduction. *J Immunol Methods 278:221*.
75. Hatakeyama, M., M. Tsudo, S. Minamoto, T. Kono, T. Doi, T. Miyata, M. Miyasaka, and T. Taniguchi. 1989. Interleukin-2 receptor beta chain gene: generation of three receptor forms by cloned human alpha and beta chain cDNA's. *Science 244:551*.
76. Migone, T. S., J. X. Lin, A. Cereseto, J. C. Mulloy, J. J. O'Shea, G. Franchini, and W. J. Leonard. 1995. Constitutively activated Jak-STAT pathway in T cells transformed with HTLV-I. *Science 269:79*.
77. Takeshita, T., H. Asao, K. Ohtani, N. Ishii, S. Kumaki, N. Tanaka, H. Munakata, M. Nakamura, and K. Sugamura. 1992. Cloning of the gamma chain of the human IL-2 receptor. *Science 257:379*.
78. Cao, X., C. A. Kozak, Y. J. Liu, M. Noguchi, E. O'Connell, and W. J. Leonard. 1993. Characterization of cDNAs encoding the murine interleukin 2 receptor (IL-2R) gamma chain: chromosomal mapping and tissue specificity of IL-2R gamma chain expression. *Proc Natl Acad Sci U S A 90:8464*.
79. Waldmann, T. A. 1989. The multi-subunit interleukin-2 receptor. *Annu Rev Biochem 58:875*.
80. Leonard, W. J., T. A. Donlon, R. V. Lebo, and W. C. Greene. 1985. Localization of the gene encoding the human interleukin-2 receptor on chromosome 10. *Science 228:1547*.
81. Leonard, W. J., J. M. Depper, M. Kanehisa, M. Kronke, N. J. Peffer, P. B. Svetlik, M. Sullivan, and W. C. Greene. 1985. Structure of the human interleukin-2 receptor gene. *Science 230:633*.
82. Ishida, N., H. Kanamori, T. Noma, T. Nikaido, H. Sabe, N. Suzuki, A. Shimizu, and T. Honjo. 1985. Molecular cloning and structure of the human interleukin 2 receptor gene. *Nucleic Acids Res 13:7579*.
83. Bohnlein, E., J. W. Lowenthal, M. Siekevitz, D. W. Ballard, B. R. Franza, and W. C. Greene. 1988. The same inducible nuclear proteins regulates mitogen activation of both the interleukin-2 receptor-alpha gene and type 1 HIV. *Cell 53:827*.
84. Leung, K., and G. J. Nabel. 1988. HTLV-1 transactivator induces interleukin-2 receptor expression through an NF-kappa B-like factor. *Nature 333:776*.
85. Cross, S. L., N. F. Halden, M. J. Lenardo, and W. J. Leonard. 1989. Functionally distinct NF-kappa B binding sites in the immunoglobulin kappa and IL-2 receptor alpha chain genes. *Science 244:466*.
86. Ruben, S., H. Poteat, T. H. Tan, K. Kawakami, R. Roeder, W. Haseltine, and C. A. Rosen. 1988. Cellular transcription factors and regulation of IL-2 receptor gene expression by HTLV-I tax gene product. *Science 241:89*.
87. Ballard, D. W., E. Bohnlein, J. A. Hoffman, H. P. Bogerd, E. P. Dixon, B. R. Franza, and W. C. Greene. 1989. Activation of the interleukin-2 receptor alpha gene: regulatory role for DNA-protein interactions flanking the kappa B enhancer. *New Biol 1:83*.
88. Toledano, M. B., D. G. Roman, N. F. Halden, B. B. Lin, and W. J. Leonard. 1990. The same target sequences are differentially important for activation of the interleukin 2 receptor alpha-chain gene in two distinct T-cell lines. *Proc Natl Acad Sci U S A 87:1830*.
89. John, S., R. B. Reeves, J. X. Lin, R. Child, J. M. Leiden, C. B. Thompson, and W. J. Leonard. 1995. Regulation of cell-type-specific interleukin-2 receptor alpha-chain gene expression: potential role of physical interactions between Elf-1, HMG-I(Y), and NF-kappa B family proteins. *Mol Cell Biol 15:1786*.
90. Gnarra, J. R., H. Otani, M. G. Wang, O. W. McBride, M. Sharon, and W. J. Leonard. 1990. Human interleukin 2 receptor beta-chain gene: chromosomal localization and identification of 5' regulatory sequences. *Proc Natl Acad Sci U S A 87:3440*.
91. Shibuya, H., M. Yoneyama, Y. Nakamura, H. Harada, M. Hatakeyama, S. Minamoto, T. Kono, T. Doi, R. White, and T. Taniguchi. 1990. The human interleukin-2 receptor beta-chain gene: genomic organization, promoter analysis and chromosomal assignment. *Nucleic Acids Res 18:3697*.
92. Cerdan, C., Y. Martin, M. Courcoul, C. Mawas, F. Birg, and D. Olive. 1995. CD28 costimulation up-regulates long-term IL-2R beta expression in human T cells through combined transcriptional and post-transcriptional regulation. *J Immunol 154:1007*.
93. Lin, J. X., N. K. Bhat, S. John, W. S. Queale, and W. J. Leonard. 1993. Characterization of the human interleukin-2 receptor beta-chain gene promoter: regulation of promoter activity by ets gene products. *Mol Cell Biol 13:6201*.

94. Lin, J. X., and W. J. Leonard. 1997. The immediate-early gene product Egr-1 regulates the human interleukin-2 receptor beta-chain promoter through noncanonical Egr and Sp1 binding sites. *Mol Cell Biol 17:3714*.
95. Noguchi, M., H. Yi, H. M. Rosenblatt, A. H. Filipovich, S. Adelstein, W. S. Modi, O. W. McBride, and W. J. Leonard. 1993. Interleukin-2 receptor gamma chain mutation results in X-linked severe combined immunodeficiency in humans. *Cell 73:147*.
96. Noguchi, M., S. Adelstein, X. Cao, and W. J. Leonard. 1993. Characterization of the human interleukin-2 receptor gamma chain gene. *J Biol Chem 268:13601*.
97. Cao, X., E. W. Shores, J. Hu-Li, M. R. Anver, B. L. Kelsall, S. M. Russell, J. Drago, M. Noguchi, A. Grinberg, E. T. Bloom, and et al. 1995. Defective lymphoid development in mice lacking expression of the common cytokine receptor gamma chain. *Immunity 2:223*.
98. Ohbo, K., N. Takasawa, N. Ishii, N. Tanaka, M. Nakamura, and K. Sugamura. 1995. Functional analysis of the human interleukin 2 receptor gamma chain gene promoter. *J Biol Chem 270:7479*.
99. Kovanen, P. E., and W. J. Leonard. 2004. Cytokines and immunodeficiency diseases: critical roles of the gamma(c)-dependent cytokines interleukins 2, 4, 7, 9, 15, and 21, and their signaling pathways. *Immunol Rev 202:67*.
100. Kondo, M., T. Takeshita, N. Ishii, M. Nakamura, S. Watanabe, K. Arai, and K. Sugamura. 1993. Sharing of the interleukin-2 (IL-2) receptor gamma chain between receptors for IL-2 and IL-4. *Science 262:1874*.
101. Noguchi, M., Y. Nakamura, S. M. Russell, S. F. Ziegler, M. Tsang, X. Cao, and W. J. Leonard. 1993. Interleukin-2 receptor gamma chain: a functional component of the interleukin-7 receptor. *Science 262:1877*.
102. Russell, S. M., A. D. Keegan, N. Harada, Y. Nakamura, M. Noguchi, P. Leland, M. C. Friedmann, A. Miyajima, R. K. Puri, W. E. Paul, and et al. 1993. Interleukin-2 receptor gamma chain: a functional component of the interleukin-4 receptor. *Science 262:1880*.
103. Russell, S. M., J. A. Johnston, M. Noguchi, M. Kawamura, C. M. Bacon, M. Friedmann, M. Berg, D. W. McVicar, B. A. Witthuhn, O. Silvennoinen, and et al. 1994. Interaction of IL-2R beta and gamma c chains with Jak1 and Jak3: implications for XSCID and XCID. *Science 266:1042*.
104. Giri, J. G., M. Ahdieh, J. Eisenman, K. Shanebeck, K. Grabstein, S. Kumaki, A. Namen, L. S. Park, D. Cosman, and D. Anderson. 1994. Utilization of the beta and gamma chains of the IL-2 receptor by the novel cytokine IL-15. *Embo J 13:2822*.
105. Kimura, Y., T. Takeshita, M. Kondo, N. Ishii, M. Nakamura, J. Van Snick, and K. Sugamura. 1995. Sharing of the IL-2 receptor gamma chain with the functional IL-9 receptor complex. *Int Immunol 7:115*.
106. Asao, H., C. Okuyama, S. Kumaki, N. Ishii, S. Tsuchiya, D. Foster, and K. Sugamura. 2001. Cutting edge: the common gamma-chain is an indispensable subunit of the IL-21 receptor complex. *J Immunol 167:1*.
107. Komschlies, K. L., K. J. Grzegorzewski, and R. H. Wiltrout. 1995. Diverse immunological and hematological effects of interleukin 7: implications for clinical application. *J Leukoc Biol 58:623*.
108. Palmer, M. J., V. S. Mahajan, L. C. Trajman, D. J. Irvine, D. A. Lauffenburger, and J. Chen. 2008. Interleukin-7 receptor signaling network: an integrated systems perspective. *Cell Mol Immunol 5:79*.
109. von Freeden-Jeffry, U., P. Vieira, L. A. Lucian, T. McNeil, S. E. Burdach, and R. Murray. 1995. Lymphopenia in interleukin (IL)-7 gene-deleted mice identifies IL-7 as a nonredundant cytokine. *J Exp Med 181:1519*.
110. Peschon, J. J., P. J. Morrissey, K. H. Grabstein, F. J. Ramsdell, E. Maraskovsky, B. C. Gliniak, L. S. Park, S. F. Ziegler, D. E. Williams, C. B. Ware, J. D. Meyer, and B. L. Davison. 1994. Early lymphocyte expansion is severely impaired in interleukin 7 receptor-deficient mice. *J Exp Med 180:1955*.
111. Namen, A. E., A. E. Schmierer, C. J. March, R. W. Overell, L. S. Park, D. L. Urdal, and D. Y. Mochizuki. 1988. B cell precursor growth-promoting activity. Purification and characterization of a growth factor active on lymphocyte precursors. *J Exp Med 167:988*.
112. Baird, A. M., R. M. Gerstein, and L. J. Berg. 1999. The role of cytokine receptor signaling in lymphocyte development. *Curr Opin Immunol 11:157*.
113. Hofmeister, R., A. R. Khaled, N. Benbernou, E. Rajnavolgyi, K. Muegge, and S. K. Durum. 1999. Interleukin-7: physiological roles and mechanisms of action. *Cytokine Growth Factor Rev 10:41*.
114. Fry, T. J., and C. L. Mackall. 2002. Interleukin-7: from bench to clinic. *Blood 99:3892*.

115. Grabstein, K. H., T. J. Waldschmidt, F. D. Finkelman, B. W. Hess, A. R. Alpert, N. E. Boiani, A. E. Namen, and P. J. Morrissey. 1993. Inhibition of murine B and T lymphopoiesis in vivo by an anti-interleukin 7 monoclonal antibody. *J Exp Med 178:257*.
116. Goodwin, R. G., S. Lupton, A. Schmierer, K. J. Hjerrild, R. Jerzy, W. Clevenger, S. Gillis, D. Cosman, and A. E. Namen. 1989. Human interleukin 7: molecular cloning and growth factor activity on human and murine B-lineage cells. *Proc Natl Acad Sci U S A 86:302*.
117. Namen, A. E., S. Lupton, K. Hjerrild, J. Wignall, D. Y. Mochizuki, A. Schmierer, B. Mosley, C. J. March, D. Urdal, and S. Gillis. 1988. Stimulation of B-cell progenitors by cloned murine interleukin-7. *Nature 333:571*.
118. Sakata, T., S. Iwagami, Y. Tsuruta, H. Teraoka, Y. Tatsumi, Y. Kita, S. Nishikawa, Y. Takai, and H. Fujiwara. 1990. Constitutive expression of interleukin-7 mRNA and production of IL-7 by a cloned murine thymic stromal cell line. *J Leukoc Biol 48:205*.
119. Gutierrez, J. C., and R. Palacios. 1991. Heterogeneity of thymic epithelial cells in promoting T-lymphocyte differentiation in vivo. *Proc Natl Acad Sci U S A 88:642*.
120. Gunji, Y., T. Sudo, J. Suda, Y. Yamaguchi, H. Nakauchi, S. Nishikawa, N. Yanai, M. Obinata, M. Yanagisawa, Y. Miura, and et al. 1991. Support of early B-cell differentiation in mouse fetal liver by stromal cells and interleukin-7. *Blood 77:2612*.
121. Link, A., T. K. Vogt, S. Favre, M. R. Britschgi, H. Acha-Orbea, B. Hinz, J. G. Cyster, and S. A. Luther. 2007. Fibroblastic reticular cells in lymph nodes regulate the homeostasis of naive T cells. *Nat Immunol 8:1255*.
122. Mazzucchelli, R., and S. K. Durum. 2007. Interleukin-7 receptor expression: intelligent design. *Nat Rev Immunol 7:144*.
123. Kondo, M., T. Takeshita, M. Higuchi, M. Nakamura, T. Sudo, S. Nishikawa, and K. Sugamura. 1994. Functional participation of the IL-2 receptor gamma chain in IL-7 receptor complexes. *Science 263:1453*.
124. Lin, J. X., T. S. Migone, M. Tsang, M. Friedmann, J. A. Weatherbee, L. Zhou, A. Yamauchi, E. T. Bloom, J. Mietz, S. John, and et al. 1995. The role of shared receptor motifs and common Stat proteins in the generation of cytokine pleiotropy and redundancy by IL-2, IL-4, IL-7, IL-13, and IL-15. *Immunity 2:331*.
125. Fry, T. J., and C. L. Mackall. 2005. The many faces of IL-7: from lymphopoiesis to peripheral T cell maintenance. *J Immunol 174:6571*.
126. Jiang, Q., W. Q. Li, F. B. Aiello, R. Mazzucchelli, B. Asefa, A. R. Khaled, and S. K. Durum. 2005. Cell biology of IL-7, a key lymphotrophin. *Cytokine Growth Factor Rev 16:513*.
127. Shaner, N. C., G. H. Patterson, and M. W. Davidson. 2007. Advances in fluorescent protein technology. *J Cell Sci 120:4247*.
128. Venturoli, D., and B. Rippe. 2005. Ficoll and dextran vs. globular proteins as probes for testing glomerular permselectivity: effects of molecular size, shape, charge, and deformability. *Am J Physiol Renal Physiol 288:F605*.
129. Asao, H., T. Takeshita, N. Ishii, S. Kumaki, M. Nakamura, and K. Sugamura. 1993. Reconstitution of functional interleukin 2 receptor complexes on fibroblastoid cells: involvement of the cytoplasmic domain of the gamma chain in two distinct signaling pathways. *Proc Natl Acad Sci U S A 90:4127*.
130. Minamoto, S., H. Mori, M. Hatakeyama, T. Kono, T. Doi, T. Ide, T. Uede, and T. Taniguchi. 1990. Characterization of the heterodimeric complex of human IL-2 receptor alpha.beta chains reconstituted in a mouse fibroblast cell line, L929. *J Immunol 145:2177*.
131. Tsudo, M., H. Karasuyama, F. Kitamura, T. Tanaka, S. Kubo, Y. Yamamura, T. Tamatani, M. Hatakeyama, T. Taniguchi, and M. Miyasaka. 1990. The IL-2 receptor beta-chain (p70). Ligand binding ability of the cDNA-encoding membrane and secreted forms. *J Immunol 145:599*.
132. Robb, R. J., W. C. Greene, and C. M. Rusk. 1984. Low and high affinity cellular receptors for interleukin 2. Implications for the level of Tac antigen. *J Exp Med 160:1126*.
133. Hamblin, A. D., and T. J. Hamblin. 2008. The immunodeficiency of chronic lymphocytic leukaemia. *Br Med Bull 87:49*.
134. Kizhatil, H., Gromeleg, A. and Albritton, L. M., 2001. Two point mutation produce infectious retrovirus bearing a green fluorescent protein-SU fusion protein. *J Virolgy 75:11881*
135. Foerster, A., Assenmacher, M., Niemoeller, M., Rankin, E., Mohaupt, M. and Richter, A. 2008. Detection and Isolation of viable mouse IL-7-secreting T cells. *J Vis Exp18:1037*
136. Metzner, C., Salmons B., Günzberg, W.H., Dangerfield, J.A. 2008. Rafts, anchors and viruses-A role for glycosylphatidylinositol anchored proteins in the modification of enveloped viruses and viral vectors. *J Virology Exp 382:12531*

6 Appendix

6.1 List of Figures

6.2 List of Tables

7 Curriculum Vitae

Personal Details

Name: MANTA, Calin-Petru

Date of Birth: 15 June 1982

Place of Birth: Bucharest (Romania)

Nationality: German

Education

1989-1990	Primary School (Nr.19 in Bucharest, Romania)
1990-1993	Primary School (Grundschule Neufrach-Salem, Germany)
1993-1994	Primary School (Grundschule Hagnau, Germany)
1994-1999	Secondary School (Sommertalschule, Meersburg, Germany) (C-level final school examination)
1999-2000	Secondary School (Wiestorschule, Überlingen, Germany) (B-level final school examination)
2000-2003	Secondary School (Justus-von-Liebig-Schule, Überlingen, Germany) (High School for nutrition science; A-level final examination)
2003-2005	Study of Biology at the University of Konstanz, Germany
2005-2009	Study of Microbiology and Genetics at the University of Vienna, Austria